Eur J Vasc Endovasc Surg (2010) 39, 179–186

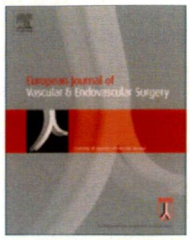

Spinal Cord Injury is Not Negligible after TEVAR for Lower Descending Aorta☆

H. Matsuda [a,*], T. Fukuda [b], O. Iritani [a], T. Nakazawa [b], H. Tanaka [a], H. Sasaki [a], K. Minatoya [a], H. Ogino [a]

[a] *Department of Cardiovascular Surgery, National Cardiovascular Center, Suita/Osaka, Japan*
[b] *Department of Radiology, National Cardiovascular Center, Suita/Osaka, Japan*

Submitted 31 August 2009; accepted 15 November 2009
Available online 3 December 2009

KEYWORDS
Thoracic aortic aneurysm;
Endovascular repair;
Stent graft;
Spinal cord injury;
Paraplegia

Abstract *Objectives:* To clarify the incidence of spinal cord injury (SCI) after thoracic endovascular aneurysm repair (TEVAR), we investigate the intercostal/lumbar arteries that supply the Adamkiewicz artery (ICA-AKA).
Patients: Among 81 patients subjected to TEVAR, we retrospectively reviewed the clinical records of 50 patients (range: 57–86 (median age: 77) years, 41 males) who underwent TEVAR for part of or the whole distal descending aorta (T7 to L2) after identification of ICA-AKA by magnetic resonance angiography (MRA) or computed tomography angiography (CTA).
Results: The 50 patients were classified into group A: 17 patients whose patent ICA-AKA was not covered, group B: 24 patients whose ICA-AKA was covered and group C: nine patients in whom no patent ICA-AKA was identified. Only three patients in group B suffered paraplegia and of them two recovered full ambulation. The estimated incidence of permanent and transient paraplegia was 3.7% in all TEVAR patients, 6.0% when part of or the entire distal aorta was covered and 12.5% when the patent ICA-AKA was covered. The length of aortic coverage in patients with paraplegia was >300 mm.
Conclusions: Paraplegia after TEVAR occurred in one of eight patients in whom the stent graft covered ICA-AKA. Long coverage of the aorta including the ICA-AKA was critical. To prevent this serious complication, identification of the ICA-AKA is crucial.

☆ This paper was presented at the XXIII Annual Meeting 3–6 September, 2009, European Society for Vascular Surgery, Oslo, Norway.

* Corresponding author at: Hitoshi Matsuda, Department of Cardiovascular Surgery, National Cardio-Vascular Center, 7-5-1 Fujishirodai, Suita/Osaka 565-8565, Japan. Tel.: +81 6 6833 5012; fax: +81 6 6872 7486.
E-mail address: hitmat@hsp.ncvc.go.jp (H. Matsuda).

1078-5884/$36
doi:10.1016/j.ejvs.2009.11.014

The incidence of spinal cord injury (SCI) after thoracic endovascular aneurysm repair (TEVAR) has been reported to vary according to the demographics of the patients.[1–20] Whether the integrity of the Adamkiewicz artery (AKA) is essential for spinal cord function is still to be investigated.[21] However, after reattachment of the intercostal/lumbar arteries, which supply AKA (ICA-AKA), or of the adjacent intercostal/lumbar arteries during thoracoabdominal aortic replacement, motor-evoked potentials (MEPs) recover.[22] TEVAR has been reported to reduce SCI.[12] In principle, the longer the length of the aorta including both landing zones that is covered by TEVAR, the larger the number of ICAs that will be sacrificed and whose revascularisation will be impossible.[23]

To clarify the incidence and cause of SCI after TEVAR, we have investigated the patency of ICA-AKA in relation to other factors which may cause SCI.

Materials/Methods

Patient demographics

In the past 27 months, of 81 patients, we performed TEVAR with Gore TAG (W. L. Gore & Associates, Flagstaff, AZ, USA) in 47 patients, Talent thoracic stent graft (Medtronic, Inc., Santa Rosa, CA, USA) in five, both TAG and Talent in one and Matsui-Kitamura (MK) stent graft in 28 patients.[24] In this study, we included 50 patients who underwent TEVAR for part of or the whole distal descending aorta after ICA-AKA was identified by magnetic resonance angiography (MRA) or computed tomography angiography (CTA). The distal descending aorta was defined as the segment between T7 and L2.[25] Fifteen patients who underwent TEVAR above T6 and 16 patients who had not undergone MRA or CTA to identify ICA-AKA were not included in this investigation.

In general, the patients were senescent, debilitated and presented co-morbidities. (Table 1) Thirty-seven patients were ≥75 years old and the median age was 77. Thirty-seven patients were in ASA class 3 or 4, and 32 patients had a history of aortic surgery (48 surgeries in total).

Of the 18 patients who had undergone AAA repair, TEVAR had been indicated more than 1 year later in 11 patients, scheduled within 3 months in five and performed simultaneously in two. Emergency TEVAR was performed in three for haemoptysis, acute aneurysm dissection and persistent back pain. They were haemodynamically stable and could undergo CTA for ICA-AKA.

In all patients, another CTA was carried out to precisely measure the aneurysm and access. CTA also revealed the patency of the left subclavian (LSCA) and bilateral internal iliac arteries (IIA). Occlusion of left IIA (LIIA) was confirmed in three patients but LSCA and right IIA (RIIA) were patent in all the patients regardless of whether total arch replacement (TAR) or AAA repair was performed.

Identification of ICA-AKA

ICA-AKA was identified by MRA in 39 and by CTA in 11 patients.

The details of contrast MRA were previously reported by Yamada et al.[26] For the CTA, an Aquilion 16 multi-detector row CT scanner (Toshiba, Tokyo, Japan) was used. To detect AKA, the reconstruction field of view was set to the area around the aorta and spine. The images were processed in a workstation (Ziostation; Amin, Tokyo, Japan). Volume-rendered images of the entire aorta were routinely generated. Multiplanar reformation (MPR) images, including oblique coronal images with craniocaudal angulations and curved planar reformation images, were reconstructed to investigate the side and level of the origin of AKA.

Diagnostic criteria for the anterior spinal artery and AKA were as previously reported.[26] We preferred MRA as CTA is disadvantageous due to the influence of the spine and lack of accurate differentiation of the AKA from the anterior radicular vein.[22] However, the selection of MRA or CTA

Table 1 Patient demographics.

Number of Patients	50			
Age	57–86 [median 77] year-old			
Gender	41 male			
ASA class	Class 2: 13, Class 3: 19, Class 4: 18			
History of aortic surgery	Root to Ascending	3		
	Arch	21	Total arch replacement	20
			TEVAR after debranch	1
	Descending		Replacement	3
			TEVAR	1
	Thoraco-abdominal	2		
	AAA	18	Replacement	17
			EVAR	1
Aortic pathology	Degenerative aneurysm	39		
	Chronic dissection	3		
	Acute dissection on aneurysm	2		
	Penetrating atherosclerotic ulcer	3		
	Anastomotic false aneurysm	3		

Table 2 Distribution of ICA-AKA.

	Right	Left	(Occlusion at origin)
Th7	0	1	
Th8	1	6	(2)
Th9	0	18	(1)
Th10	1	10	
Th11	0	7	(1)
Th12	2	4	(2)
L1	0	1	
L2	0	0	
Total	4	47	(6)

ICA-AKA: intercostal/lumbar arteries which supplies Adamkiewicz artery.

depended on the availability of the equipment. CTA was used in all three emergency cases.

When AKA was not identified by MRA, it was diagnosed as 'absent' ($n = 3$). In 47 patients, 51 ICA-AKAs were identified (Table 2). In four patients, there were double ICA-AKAs. Occlusion of ICA-AKA at its origin was diagnosed in six patients, in all of them on the left side. When the ICA-AKA was occluded, blood supply from adjacent intercostal or lumbar arteries was suspected to be significant. However, we were unable to distinguish the critical collateral flow to AKA.

TEVAR

To create a landing zone, a carotid–subclavian bypass was performed in two and visceral vessel bypass was performed in one. In nine patients who had extensive/multiple aneurysm(s) from the aortic arch to the descending aorta, TAR was performed using elephant trunk (ET) implantation. Regarding patients who had a history of aortic surgery, an artificial graft was used to create a proximal landing zone in 19 and a distal landing zone in three.

In all patients, TEVAR was carried out under general anaesthesia. The access route for TEVAR was a native artery in 35, an iliac conduit in 13 and a graft limb or a side branch of AAA graft in two patients.

MEP monitoring and cerebrospinal fluid drainage

In all patients trans-cranial MEPs were monitored during TEVAR and a cerebrospinal fluid drainage (CSFD) tube was placed before TEVAR in 31 patients.

Immediately after the stent graft was placed, the mean blood pressure was raised above 80 mmHg and MEP was monitored every 5 min. When the amplitude of MEPs decreased under general anaesthesia, or when symptoms and signs of SCI were noted during the postoperative period, CSFD (<15 cmH_2O) was started with the infusion of methylprednisolone (30 mg kg^{-1} bolus and 5.4 mg kg^{-1} h^{-1} for 23 h followed by 2.7 mg kg^{-1} h^{-1} for 2 days) and naloxone (1200 μg day^{-1}). Intensive spinal care with CSFD, methylprednisolone and naloxone was continued for 72 h if the symptom did not resolve or was discontinued 24 h after full recovery.

CSFD was started only after paraplegia or a decrease of less than 25% of the amplitude of MEPs was noted. CSFD was not indicated as a prophylactic measure after TEVAR.

Measurement of the aortic length

The length of 'proximal uncovered aorta' (from LSCA to stent graft), 'aortic coverage' by stent graft and 'distal uncovered aorta' (from stent graft to coeliac axis (CA)) was measured on CTA using curved planar reformation images processed in a workstation (GE Advantage workstation 4.3).

After TAR with a multibranch graft, the length of aortic coverage was measured from the distal anastomosis. This site coincided with the origin of ET and was several centimetres distal to the branch graft of LSCA. When ET was installed, the proximal edge of the stent graft was positioned inside the multibranch graft and not only inside ET. After replacement of the descending or the thoracoabdominal aorta, the position of LSCA and/or CA served as the point of reference for the measurement.

Statistical analysis

Values are the mean ± SD. Data were analysed using the chi-square test for categorical variables, and continuous variables were examined using analysis of variance (ANOVA). The level of statistical significance was set at $p < 0.05$.

Results

Mortality and morbidity

Initial success of TEVAR was achieved in all patients except for two patients with Type I endoleaks detected by CTA who were successfully treated by a repeat TEVAR. No operative (30 days) death was encountered. Injury and occlusion of access arteries occurred in one. Two patients were complicated with cerebral embolism due to the guidewire pull-through technique and atrial fibrillation.

The following three patients were complicated with paraplegia: Patient 1 was a 59-year-old man with a history of closure of ventricular septal defect, aortic valve replacement and repair of a Valsalva sinus aneurysm. He also suffered from liver cirrhosis. He developed aneurysmal dilatation of the whole thoracic aorta and underwent TAR with ET installation as the first-stage repair. MRA revealed the AKA arose from the left Th9-ICA. TEVAR with Gore TAG was performed 5 weeks later from ET (Z3) to T11. The iliac conduit was connected to the right common iliac artery but the haemostasis was time consuming because of obvious coagulopathy due to liver cirrhosis. Paraplegia was confirmed 24 h after TEVAR after the patient suffered much pain. Despite treatment for SCI, the patient could not ambulate. Retroperitoneal haematoma had to be removed twice. He eventually died from methicillin-resistant *Staphylococcus aureus* (MRSA) mediastinitis 4 months after TEVAR. The length of aortic coverage from the origin of ET to the distal flair was 325 mm.

Patient 2 was an 81-year-old man with ascending, arch and descending aorta aneurysms. MRA revealed the AKA branching from the left Th9-ICA. Four weeks after TAR with ET installation, TEVAR with TAG was performed from ET (Z3) to T12 (Fig. 1). The iliac conduit was required and

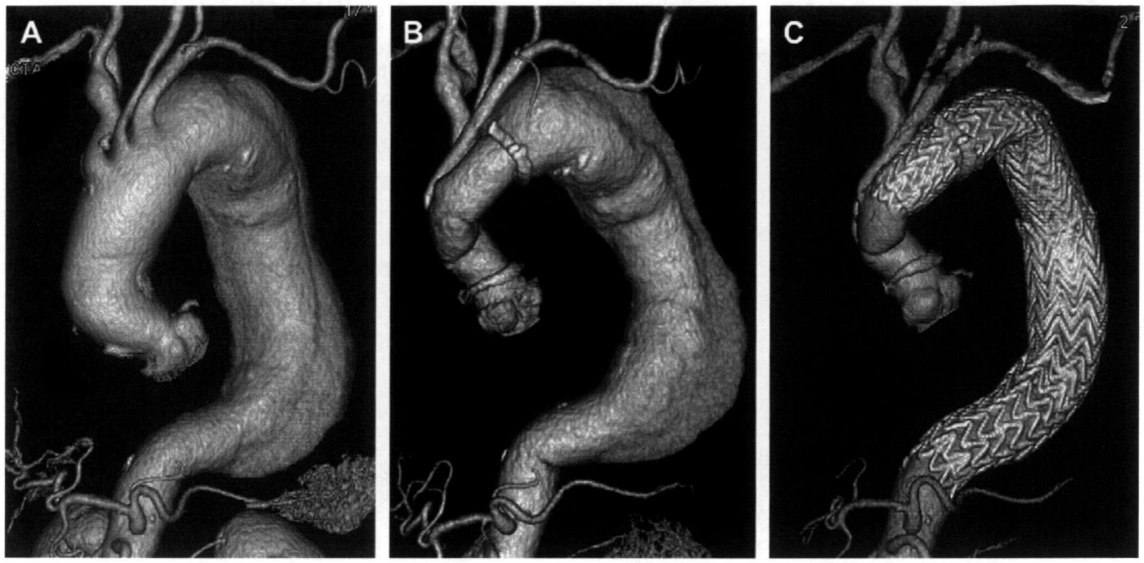

Figure 1 Sequence of CTA in Patient 2. Panel A: Preoperative, Panel B: After total arch replacement, Panel C: After TEVAR.

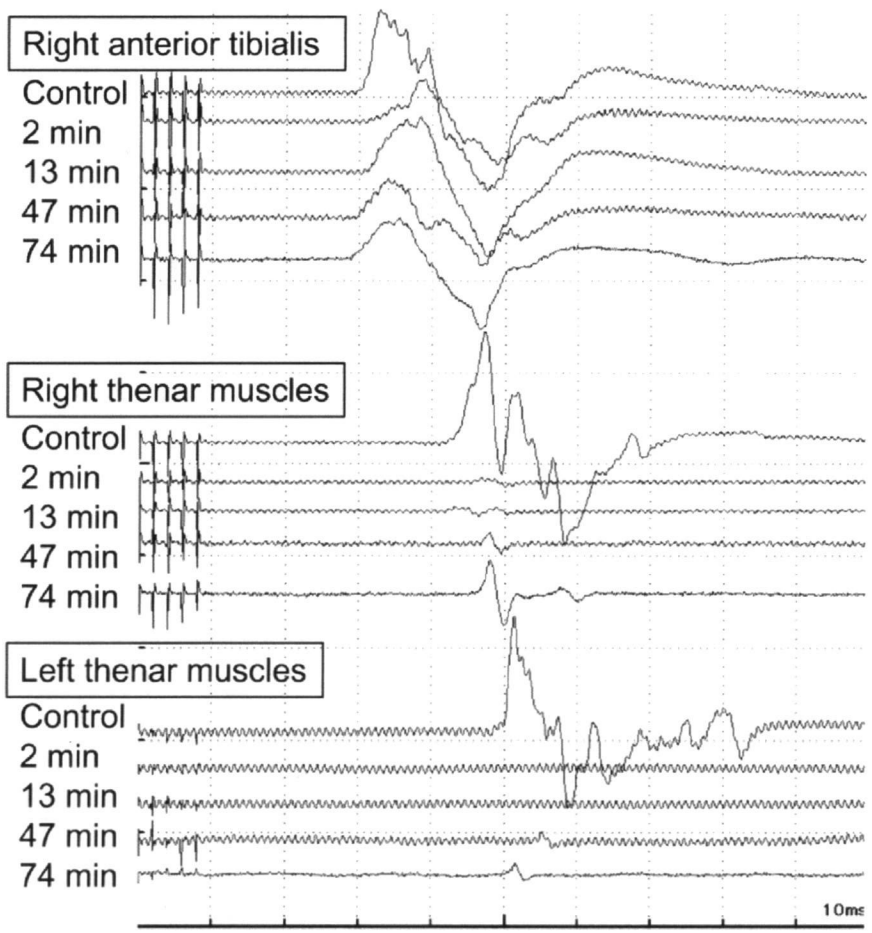

Figure 2 Sequence of MEPs in Patient 3. MEPs of the right anterior tibialis and both thenar muscles before TEVAR over Th9-ICA (control) and 2, 13, 47, and 74 minutes after TEVAR.

haemostasis took a long time due to co-existing consumption coagulopathy caused by aortic lesions. Six hours after TEVAR, the patient suddenly complained of back pain and paraplegia was confirmed. One hour after intensive spinal treatment, he could move his legs and on the next morning he could walk. The retroperitoneal, femoral and brachial haematomas were removed twice. The length of aortic coverage was 302 mm.

Patient 3 was a 78-year-old woman who had undergone TEVAR (Z3 to T7) for a proximal descending aortic aneurysm 6 months earlier. MRA revealed the ICA-AKA branching from the left Th9-ICA. Due to the rapid growth of the distal descending aortic aneurysm, TEVAR was performed again from the previous stent graft to L1. The CA was closed to create a distal landing zone. Immediately after the deployment over the Th9-ICA, the MEPs of both thenar muscles diminished and the amplitude of the MEPs of the right anterior tibialis decreased about 50% from the control amplitude (Fig. 2). Despite treatment for SCI, ankle dorsiflexion was slight when she awoke from anaesthesia. Intensive spinal care was continued and she gradually gained muscle strength within 3 h after TEVAR. On the following morning she could ambulate. The length of aortic coverage after the first TEVAR was 157 mm and was extended to 308 mm by the second TEVAR.

Incidence of paraplegia

The 50 patients were classified into group A: 17 patients whose patent ICA-AKA was not covered by TEVAR, group B: 24 patients whose ICA-AKA was covered by TEVAR and group C: nine patients in whom no patent ICA-AKA was identified. Group C included six patients whose ICA-AKA occluded at its origin and three patients whose ICA-AKA was absent.

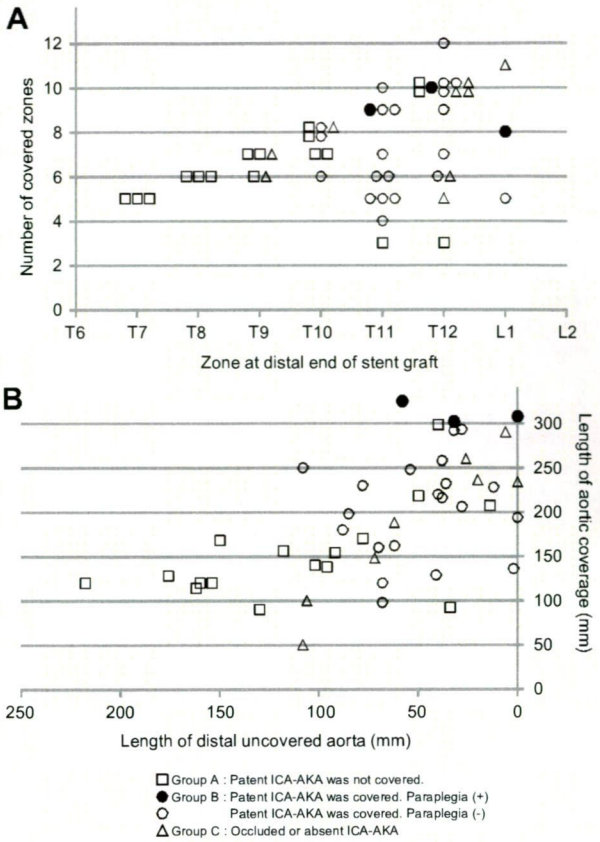

Figure 3 Distribution of patients with paraplegia in accordance with covered aorta and distal uncovered aorta expressed as number of aortic zones (Panel A) and measured length (Panel B).

Table 3 Comparison of patients with and without paraplegia.

	Paraplegia $N = 3$	No paraplegia $N = 47$	p
Age (year-old)	72.7 ± 11.9	76.1 ± 6.1	.3736
Male gender	2 (67%)	39 (83%)	.5094
ASA classification	3.7 ± 0.6	3.1 ± 0.8	.2026
Renal dysfunction	1 (33%)	18 (38%)	.3362
History of aortic repair (descending, thoracoabdominal, abdominal)	1 (33%)	19 (40%)	.8060
LSCA patency	3 (100%)	47 (100%)	–
RIIA patency	3 (100%)	47 (100%)	–
LIIA patency	3	44	.5359
Op time (minutes)	252 ± 117	141 ± 76	.0200
Blood loss (ml)	557 ± 274	363 ± 423	.4482
Use of an iliac conduit	2 (67%)	15 (32%)	.2335
Zones of aortic coverage	9 ± 1	7.2 ± 2.2	.1691
Proximal uncovered aorta (mm)	0	36 ± 49	.2191
Aortic coverage (mm)	312 ± 12	179 ± 64	.0009
Distal uncovered aorta (mm)	30 ± 29	72 ± 52	.1839
Hypotension	2 (67%)	3 (6%)	.0116

LSCA: Left subclavian artery, R(L)IIA: Right internal iliac artery.

Table 4 Reported incidence of spinal cord injury (SCI).

	Patients	Location	N	SCI	
Criado, 2002	TEVAR	Arch-descending	47	0	(0.0%)
Bergeron, 2003	TEVAR	Descending	38	0	(0.0%)
Czerny, 2004	TEVAR	Descending	54	0	(0.0%)
Orend, 2003	TEVAR	Various	74	2	(2.7%)
Mitchell, 1999	TEVAR	n/d	103	3	(2.9%)
Makaroun, 2005	TAG phase II	Various	142	4	(3.0%)
Ellozy, 2003	TEVAR	Descending	84	3	(3.6%)
Morales, 2007	TEVAR	n/d	186	7	(3.8%)
Bell, 2003	TEVAR	Various	67	3	(4.0%)
Greenberg, 2008	TEVAR	TAAA	352	15	(4.3%)
Gravereaux, 2001	TEVAR	Descending	53	3	(5.7%)
Greenberg, 2005	TXI & TXII	Various	100	6	(6.0%)
Sandroussi, 2007	TEVAR	n/d	65	4	(6.2%)
Cheung, 2005	TEVAR	Various	75	5	(6.5%)
Amabile, 2008	TEVAR	Descending	67	5	(7.5%)
Feezor, 2008	TEVAR	n/d	326	33	(10.0%)

The three patients who developed paraplegia were in group B, that is, ICA-AKA was covered by TEVAR. The estimated incidence of permanent and transient paraplegia was 3.7% in all patients subjected to TEVAR (81 patients), 4.5% in patients in whom part or the entire distal aorta was covered, regardless of ICA-AKA identification by MRA (66 patients) and 6.0% in those whose ICA-AKA was identified (50 patients, groups A, B and C). The incidence increased to 12.5% only when the patent ICA-AKA was covered by TEVAR (24 patients, group B).

Comparison of patients with and without paraplegia after TEVAR showed that the operation time and the length of aortic coverage were significantly longer in those with paraplegia (Table 3). Episodes of hypotension below 80 mmHg for more than 10 min during and after surgery were more frequent in patients with paraplegia. No difference was found in the patency rate of LSCA[27] and IIA. Other risk factors previously reported[28] such as the abdominal aortic surgery and the renal dysfunction showed no difference.

Fig. 3 shows the occurrence of paraplegia in relation to aortic coverage and distal aortic uncoverage length. When these were divided into zones, the stent grafts in the three patients with paraplegia were placed at T11 or distal to it and covered more than eight zones. Fourteen patients without paraplegia had the same range of intervened zones (Fig. 3A). In the three patients with paraplegia, the length of aortic coverage was more than 300 mm. The length of distal uncovered aorta was within 60 mm. Four other patients whose length of aortic coverage was between 270 mm and 300 mm and the length of distal uncovered aorta was less than 60 mm did not experience paraplegia (Fig. 3B).

Discussion

We have reported the low risk of paraplegia for patients subjected to descending and thoraco-abdominal aorta open repair by combined use of AKA identification by MRA and MEP measurement.[22] The risk of paraplegia has been considered to be lower after TEVAR than after open repair, but the incidence of SCI in the previous reports varied (Table 4). This variation might be due to differences in case mix as the area subjected to TEVAR was not the same and was not specified in some of the reports.[23]

The theoretical advantages of TEVAR concerning protection of the spinal cord are the maintenance of distal perfusion, stable haemodynamics and no reperfusion of the spinal cord.[12] However, additional ICAs are sacrificed for the landing zones and revascularisation of the ICAs is impossible. Paraplegia occurs after TEVAR when the arteries that supply the spinal cord are sacrificed, as well as after a period of hypotension or as a result of emboli from aortic atheromatous lesions.[29]

We encountered paraplegia in three patients whose patent ICA-AKA was covered and the length of aortic coverage was more than 300 mm. The rate of permanent and transient paraplegia was 12.5% (1/8), when the patent ICA-AKA was covered by TEVAR. This result was in agreement with that of a previous study showing that SCI occurred in 9.1% of the patients with occlusion of the ICA-AKA.[13] The authors did not encounter paraplegia in patients whose ICA-AKA was patent. This fact is also relevant to our result as none of our patients, whose ICA-AKA was already occluded at its origin before TEVAR or was absent, experienced paraplegia.

The spinal cord blood supply depends on many interchangeable collateral arteries that supply the anterior spinal cord artery, rather than a single dominant AKA.[21] However, the importance of the patency of the ICA-AKA during TEVAR[13] and the restoration of blood flow in the spinal cord after revascularisation of ICA-AKA at the aortic replacement have been reported.[22] Patency of ICA-AKA is sufficient to prevent paraplegia and occlusion of the patent ICA-AKA is critical. To preserve the patency of ICA-AKA, this should be identified preoperatively to allow the creation of an adequate landing zone.[12]

The rate of paraplegia, 12.5%, means that 87.5% (7/8) patients did not develop paraplegia after the coverage of patent ICA-AKA. Between three patients who suffered paraplegia and 21 patients who did not in group B, the threshold of the length of aortic coverage was 300 mm. The length of aortic coverage has been described as a risk for SCI in previous reports.[13,30] Amabile et al. reported that

205 mm was the critical length of aortic coverage for SCI.[18] Feezor et al. described that both the extent (>200 mm) and distal location of aortic coverage (20 mm from CA) were associated with an increased risk for SCI.[16]

We tried to locate the critical segment for paraplegia by dividing the aorta into zones but the length measured by CTA demonstrated the critical length of aortic coverage more clearly. This particular threshold, 300 mm, might vary in the future as experience accumulates and the index is modified, for instance, according to height. Nevertheless, it can be emphasised that long aortic coverage is another important risk factor for paraplegia. Long coverage of the aorta including the patent ICA-AKA is critical.

We found intra-operative coagulopathy related to prolonged operation time and postoperative retroperitoneal bleeding in patient 1 and patient 2. Hypotension associated with retroperitoneal bleeding contributes to SCI.[6] Consumption coagulopathy is another risk which is heightened by long coverage of the aorta.

Paraplegia occurred when the stent graft covered the zones at T11 or was placed less than 60 mm from CA. It can be concluded that the zones above T10 or a distance of more than 60 mm from CA are safe. However, the length of distal uncovered aorta would only express the probability of the occlusion of the ICA-AKA according to its distribution. The length of distal uncovered aorta might be less significant than the closure of the ICA-AKA or the length of aortic coverage.

Similarly, high percentages of paraplegia, 12.5% and 14.3%, after TEVAR were reported in patients with prior AAA repair.[12,20] In our series, a history of abdominal, thoraco-abdominal, or descending aneurysm repair was not a significant risk for paraplegia. However, AAA repair sacrifices several pairs of lumbar arteries that significantly contribute to spinal cord perfusion and/or IIA, which are the possible sources of direct or collateral blood flow to spinal arteries. Indeed, previous AAA repair was described as a risk factor in various other reports.[2,6,12,27,31]

Limitations of this study include the retrospective review of prospectively collected data, the retrospective measurement of aortic length and the small number of patients. Further accumulation of patients treated by TEVAR after identification of ICA-AKA is crucial for more precise diagnosis of the risk for paraplegia after TEVAR.

Conclusions

Paraplegia after TEVAR occurred in 1 of 8 (12.5%) patients in whom the stent graft covered the distal descending aorta below Th7. Long (>300 mm) coverage of the aorta including the ICA-AKA is a critical risk factor for SCI and paraplegia. To prevent this serious complication, it is imperative to identify the ICA-AKA before performing TEVAR.

Conflict of Interest/Funding

None.

Acknowledgement

We express our sincere appreciation to Dr. Naoaki Yamada and Dr. Masahiro Higashi (from the Department of Radiology, National Cardiovascular Center), who contributed to the clear visualisation of the Adamkiewicz artery by MRA and CTA.

References

1 Mitchell RS, Miller DC, Dake MD, Semba CP, Moore KA, Sakai T. Thoracic aortic aneurysm repair with an endovascular stent graft: the "first generation" *Ann Thorac Surg* 1999;**67**:1971–4.
2 Gravereaux EC, Faries PL, Burks JA, Latessa V, Spielvogel D, Hollier LH, et al. Risk of spinal cord ischemia after endograft repair of thoracic aortic aneurysms. *J Vasc Surg* 2001;**34**:997–1003.
3 Criado FJ, Clark NS, Barnatan MF. Stent graft repair in the aortic arch and descending thoracic aorta: a 4-year experience. *J Vasc Surg* 2002;**36**:1121–8.
4 Ellozy SH, Carroccio A, Minor M, Jacobs T, Chae K, Cha A, et al. Challenges of endovascular tube graft repair of thoracic aortic aneurysm: midterm follow-up and lessons learned. *J Vasc Surg* 2003;**38**:676–83.
5 Orend KH, Scharrer-Pamler R, Kapfer X, Kotsis T, Görich J, Sunder-Plassmann L. Endovascular treatment in diseases of the descending thoracic aorta: 6-year results of a single center. *J Vasc Surg* 2003;**37**:91–9.
6 Cheung AT, Pochettino A, McGarvey ML, Appoo JJ, Fairman RM, Carpenter JP, et al. Strategies to manage paraplegia risk after endovascular stent repair of descending thoracic aortic aneurysms. *Ann Thorac Surg* 2005;**80**:1280–8.
7 Bell RE, Taylor PR, Aukett M, Sabharwal T, Reidy JF. Mid-term results for second-generation thoracic stent grafts. *Br J Surg* 2003;**90**:811–7.
8 Bergeron P, De Chaumaray T, Gay J, Douillez V. Endovascular treatment of thoracic aortic aneurysms. *J Cardiovasc Surg (Torino)* 2003;**44**:349–61.
9 Czerny M, Cejna M, Hutschala D, Fleck T, Holzenbein T, Schoder M, et al. Stent-graft placement in atherosclerotic descending thoracic aortic aneurysms: midterm results. *J Endovasc Ther* 2004;**11**:26–32.
10 Makaroun MS, Dillavou ED, Kee ST, Sicard G, Chaikof E, Bavaria J, et al. Endovascular treatment of thoracic aortic aneurysms: results of the phase II multicenter trial of the GORE TAG thoracic endoprosthesis. *J Vasc Surg* 2005;**41**:1–9.
11 Greenberg RK, O'Neill S, Walker E, Haddad F, Lyden SP, Svensson LG, et al. Endovascular repair of thoracic aortic lesions with the Zenith TX1 and TX2 thoracic grafts: intermediate-term results. *J Vasc Surg* 2005;**41**:589–96.
12 Baril DT, Carroccio A, Ellozy SH, Palchik E, Addis MD, Jacobs TS, et al. Endovascular thoracic aortic repair and previous or concomitant abdominal aortic repair: is the increased risk of spinal cord ischemia real? *Ann Vasc Surg* 2006;**20**:188–94.
13 Kawaharada N, Morishita K, Kurimoto Y, Hyodoh H, Ito T, Harada R, et al. Spinal cord ischemia after elective endovascular stent-graft repair of the thoracic aorta. *Eur J Cardiothorac Surg* 2007;**31**:998–1003.
14 Morales JP, Taylor PR, Bell RE, Chan YC, Sabharwal T, Carrell TW, et al. Neurological complications following endoluminal repair of thoracic aortic disease. *Cardiovasc Intervent Radiol* 2007;**30**:833–9.
15 Sandroussi C, Waltham M, Hughes CF, May J, Harris JP, Stephen MS, et al. Endovascular grafting of the thoracic aorta, an evolving therapy: ten-year experience in a single centre. *ANZ J Surg* 2007;**77**:974–80.
16 Feezor RJ, Martin TD, Hess Jr PJ, Daniels MJ, Beaver TM, Klodell CT, et al. Extent of aortic coverage and incidence of spinal cord ischemia after thoracic endovascular aneurysm repair. *Ann Thorac Surg* 2008;**86**:1809–14.
17 Greenberg RK, Lu Q, Roselli EE, Svensson LG, Moon MC, Hernandez AV, et al. Contemporary analysis of descending

thoracic and thoracoabdominal aneurysm repair: a comparison of endovascular and open techniques. *Circulation* 2008;**118**: 808–17.
18 Amabile P, Grisoli D, Giorgi R, Bartoli JM, Piquet P. Incidence and determinants of spinal cord ischaemia in stent-graft repair of the thoracic aorta. *Eur J Vasc Endovasc Surg* 2008;**35**:455–61.
19 Hnath JC, Mehta M, Taggert JB, Stembach Y, Roddy SP, Kreienberg PB, et al. Strategies to improve spinal cord ischemia in endovascular thoracic aortic repair: outcomes of a prospective cerebrospinal fluid drainage protocol. *J Vasc Surg* 2008;**48**:836–40.
20 Schlösser FJ, Verhagen HJ, Lin PH, Verhoeven EL, van Herwaarden JA, Moll FL, et al. TEVAR following prior abdominal aortic aneurysm surgery: increased risk of neurological deficit. *J Vasc Surg* 2009;**49**:308–14.
21 Griepp RB, Ergin MA, Galla JD, Lansman S, Khan N, Quintana C, et al. Looking for the artery of Adamkiewicz: a quest to minimize paraplegia after operations for aneurysms of the descending thoracic and thoracoabdominal aorta. *J Thorac Cardiovasc Surg* 1996;**112**:1202–13.
22 Ogino H, Sasaki H, Minatoya K, Matsuda H, Yamada N, Kitamura S. Combined use of adamkiewicz artery demonstration and motor-evoked potentials in descending and thoracoabdominal repair. *Ann Thorac Surg* 2006;**82**:592–6.
23 Bicknell CD, Riga CV, Wolfe JH. Prevention of paraplegia during thoracoabdominal aortic aneurysm repair. *Eur J Vasc Endovasc Surg* 2009;**37**:654–60.
24 Sanada J, Matsui O, Terayama N, Kobayashi S, Minami T, Kurozumi M, et al. Clinical application of a curved nitinol stent-graft for thoracic aortic aneurysms. *J Endovasc Ther* 2003;**10**: 20–8.
25 Ishimaru S. Endografting of the aortic arch. *J Endovasc Ther* 2004;**11**(Suppl 2):II62–II71.
26 Yamada N, Takamiya M, Kuribayashi S, Okita Y, Minatoya K, Tanaka R. MRA of the Adamkiewicz artery: a preoperative study for thoracic aortic aneurysm. *J Comput Assist Tomogr* 2000;**24**: 362–8.
27 Cooper DG, Walsh SR, Sadat U, Noorani A, Hayes PD, Boyle JR. Neurological complications after left subclavian artery coverage during thoracic endovascular aorticrepair: a systematic review and meta-analysis. *J Vasc Surg* 2009;**49**: 1594–601.
28 Buth J, Harris PL, Hobo R, van Eps R, Cuypers P, Duijm L, et al. Neurologic complications associated with endovascular repair of thoracic aortic pathology: incidence and risk factors. a study from the European Collaborators on Stent/Graft Techniques for Aortic Aneurysm Repair (EUROSTAR) registry. *J Vasc Surg* 2007; **46**:1103–10.
29 Carroccio A, Marin ML, Ellozy S, Hollier LH. Pathophysiology of paraplegia following endovascular thoracic aortic aneurysm repair. *J Card Surg* 2001;**11**:359–66.
30 Greenberg R, Resch T, Nyman U, Lindh M, Brunkwall J, Brunkwall P, et al. Endovascular repair of descending thoracic aortic aneurysms: an early experience with intermediate-term follow-up. *J Vasc Surg* 2000;**31**:147–56.
31 Mitchell RS, Miller DC, Dake MD. Stent-graft repair of thoracic aortic aneurysms. *Semin Vasc Surg* 1997;**10**:257–71.

RESEARCH ARTICLE

Human Mutation

OFFICIAL JOURNAL
HGVS
HUMAN GENOME VARIATION SOCIETY
www.hgvs.org

Mutation of *ACTA2* Gene as an Important Cause of Familial and Nonfamilial Nonsyndromatic Thoracic Aortic Aneurysm and/or Dissection (TAAD)

Hiroko Morisaki,[1] Koichi Akutsu,[2] Hitoshi Ogino,[3] Norihiro Kondo,[4] Itaru Yamanaka,[1] Yoshiaki Tsutsumi,[2] Tsuyoshi Yoshimuta,[2] Toshiya Okajima,[2] Hitoshi Matsuda,[3] Kenji Minatoya,[3] Hiroaki Sasaki,[3] Hiroshi Tanaka,[3] Hatsue Ishibashi-Ueda,[5] and Takayuki Morisaki[1,6]*

[1]*Department of Bioscience, National Cardiovascular Center Research Institute, Osaka, Japan;* [2]*Department of Cardiovascular Medicine, National Cardiovascular Center, Osaka, Japan;* [3]*Department of Cardiovascular Surgery, National Cardiovascular Center, Osaka, Japan;* [4]*Department of Cardiovascular Surgery, Aomori Municipal Hospital, Aomori, Japan;* [5]*Department of Pathology, National Cardiovascular Center, Osaka, Japan;* [6]*Department of Molecular Pathophysiology, Osaka University Graduate School of Pharmaceutical Sciences, Osaka, Japan*

Communicated by Nancy B. Spinner

Received 26 February 2009; accepted revised manuscript 17 June 2009.
Published online 7 July 2009 in Wiley InterScience (www.interscience.wiley.com). DOI 10.1002/humu.21081

ABSTRACT: Approximately 20% of aortic aneurysm and/or dissection (AAD) cases result from inherited disorders, including several systemic and syndromatic connective-tissue disorders, such as Marfan syndrome, Ehlers-Danlos syndrome, and Loeys-Dietz syndrome, which are caused by mutations in the *FBN1*, *COL3A1*, and *TGFBR1* and *TGFBR2* genes, respectively. Nonsyndromatic AAD also has a familial background, and mutations of the *ACTA2* gene were recently shown to cause familial AAD. In the present study, we conducted sequence analyses of the *ACTA2* gene in 14 unrelated Japanese patients with familial thoracic AAD (TAAD), and in 26 with sporadic and young-onset TAAD. Our results identified three mutations of *ACTA2*, two novel [p.G152_T205del (c.616+1G>T), p.R212Q] and one reported (p.R149C), in the 14 patients with familial TAAD, and a novel mutation (p.Y145C) of *ACTA2* in the 26 sporadic and young-onset TAAD patients, each of which are considered to be causative for TAAD. Some of the clinical features of these patients were the same as previously reported, whereas others were different. These findings confirm that *ACTA2* mutations are important in familial TAAD, while the first sporadic and young-onset TAAD case with an *ACTA2* mutation was also identified.
Hum Mutat 30:1406–1411, 2009. © 2009 Wiley-Liss, Inc.

KEY WORDS: aortic aneurysm and dissection; AAD; smooth muscle actin

Introduction

Patients with an aortic aneurysm and/or dissection (AAD) have significant cardiovascular morbidity and mortality. Approximately 20% of those aneurysms result from inherited disorders, including several systemic and syndromatic connective-tissue disorders, such as Marfan syndrome, Ehlers-Danlos syndrome, and Loeys-Dietz syndrome, which are caused by mutations in the *FBN1* (MIM# 134797) [Dietz et al., 1991], *COL3A1* (MIM# 120180) [Superti-Furga et al., 1988], and *TGFBR1* (MIM# 190181), and *TGFBR2* genes (MIM# 190182) [Mizuguchi et al., 2004; Loeys et al., 2005], respectively. Familial aggregation studies have revealed that up to 20% of nonsyndromatic AAD cases have a familial background, inherited primarily in an autosomal dominant manner [Biddinger et al., 1997; Coady et al., 1999; Albornoz et al., 2006; Pannu et al., 2006], with several identified genetic loci linked to nonsyndromatic AAD. In addition, a bicuspid aortic valve is known to be present in as much as 1 to 2% of the general population, and it has been noted that such a condition can deteriorate blood flow and may cause AAD. Indeed, mutations of *NOTCH1* (MIM# 190198) were reported to cause a spectrum of developmental aortic valve anomalies, including bicuspid valve and calcification leading to aortic diseases [Garg et al., 2005]. Recently, heterozygous mutations affecting two structural maintenance of chromosomes (SMC) contractile proteins, MYH11 and ACTA2, were identified as causing familial thoracic aortic aneurysms leading to acute aortic dissections [Zhu et al., 2006; Guo et al., 2007]. Although *MYH11* (MIM# 160745) mutations seem to be rare and only five mutations have been reported thus far [Zhu et al., 2006; Pannu et al., 2007], Guo et al. [2007] reported nine *ACTA2* (MIM# 102620) mutations in 14 pedigrees among 97 analyzed families with thoracic AAD (TAAD) and claimed that *ACTA2* mutations are the most common cause of familial TAAD yet found, responsible for 14% of reported cases. They also pointed out that persistent livedo reticularis, which is caused by constriction occlusion of deep dermal capillaries, was present in most of the affected individuals.

In order to assess the clinical spectra and genetic contributions associated with mutations in *ACTA2*, we performed sequence analysis of this gene in 14 familial cases and 26 sporadic and young-onset cases with TAAD, and identified four mutations, three novel and one reported. We then compared the clinical symptoms of our patients to those described in previous reports. In one of our patients, who carried the same mutation as reported in a previous study, livedo reticularis and an iris cyst were noted. The other two patients in the pedigrees each had a strong family history of TAAD or thoracoabdominal aortic aneurysm (TAAA),

Additional Supporting Information may be found in the online version of this article.

*Correspondence to: Takayuki Morisaki, MD, PhD, Department of Bioscience, National Cardiovascular Center Research Institute, 5-7-1 Fujishirodai, Suita, Osaka, Japan. E-mail: morisaki@ri.ncvc.go.jp

though they did not show other symptoms that were described in that previous report. Another case of sporadic and young-onset TAAD also showed no specific features, though the patient was obese. These characteristics demonstrate the variable clinical features present in patients with *ACTA2* mutations.

Materials and Methods

Study Subjects

For the present study, 14 unrelated Japanese patients with TAAD and at least one first-degree relative suffering from aortic disease without any known genetic syndromatic feature in any family members (familial nonsyndromatic TAAD) were initially recruited from patients referred to the National Cardiovascular Center (Japan), between July 2005 and July 2008. Next, another 26 Japanese patients with sporadic and young-onset TAAD, whose age of onset was younger than 50 years, who were without any known genetic syndromatic feature, and did not have any family history of AAD, were also recruited from patients referred to National Cardiovascular Center (Japan) between July 2005 and July 2008. All were screened in advance for mutations of the *FBN1*, *FBN2*, *TGFBR1*, and *TGFBR2* genes by sequencing all exons and flanking intronic regions to rule out genetic disorders caused by those genetic mutations. In one of the pedigrees (Family 3), five other family members including two patients were also added before our analysis to confirm cosegregation of the mutation with the clinical phenotype. Data regarding the clinical phenotypes of the patients were collected from medical records or obtained by a physical examination. All participants gave written informed consent for genetic analyses prior to participating in the study protocol, which was approved by the Ethics Committee of the National Cardiovascular Center.

Mutation Analysis

Genomic DNA was extracted from leukocytes isolated from peripheral blood samples using an NA-3000 (Kurabo, Osaka, Japan), according to the manufacturer's protocol. All exons and flanking intronic regions of the *ACTA2* gene were amplified by polymerase chain reaction (PCR) using AmpliTaq Gold polymerase (Applied Biosystems, Foster City, CA) and an ABI 9700 thermal cycler (Applied Biosystems). The sequences of the PCR primers have been described elsewhere [Guo et al., 2007]. PCR products were purified with ExoSAP-IT (USB Corporation, Cleveland, OH) and both strands sequenced using BigDye Terminator chemistry version 1.1, followed by analysis using an ABI genetic analyzer 3730 with sequence analysis software (Applied Biosystems). PCR amplifications and direct sequencing analyses were performed according to the manufacturer's instructions. For the proband in Family 2, total RNA from an aortic tissue sample was isolated using TRIzol (Invitrogen, Carlsbad, CA) reagent, then reverse-transcribed using SuperScript III reverse transcriptase (Invitrogen) and random primers prior to RT-PCR analysis, according to the supplier's instructions. RT-PCR primers were designed to amplify a fragment containing the whole coding sequence of *ACTA2* cDNA, including parts of the 5′- and 3′-untranslated regions. RT-PCR analysis was also performed using primers located in exon 5 and exon 7 to assess the amount of transcripts with skipping of exon 6. Mutation numbering was performed based on the reference cDNA sequence (NM_001613.1), where +1 corresponded to the nucleotide A of ATG, the translation initiation codon (www.hgvs.org/mutnomen). Illustrations of the protein structures of ACTA2 and interacting proteins were created using a graphics program (Swiss-Pdb Viewer, Deep View v4.0) [Guex and Peitsch, 1988] based on structural data deposited in the Protein Data Bank (PDB-ID 1NM1).

Results

In 3 out of 14 probands diagnosed with familial nonsyndromatic TAAD, we identified three mutations, two novel and one reported, considered to have effects on the amino acid sequence of ACTA2. In the study of 26 sporadic and young-onset TAAD patients, we identified one novel missense mutation affecting a highly-conserved amino acid that would be indispensable for ligand binding. None of those TAAD patients had a bicuspid aortic valve.

Family 1

c.445C>T (p.Arg149Cys in exon 5), which was the same mutation of *ACTA2* described as 492C>T (p.Arg149Cys) in a previous report, was detected in a female proband (Patient II:2, index) in Family 1, who had a positive family history of aortic dissection and iris cysts. She had been an active amateur tennis player in her teens. Her first pregnancy, 4 years prior to referral, was uneventful with a spontaneous vaginal delivery at term. At the age of 31 years, she experienced an acute thoracoabdominal aortic dissection (Stanford B type) during spontaneous vaginal delivery of her second child (male, 40 weeks, 2,680 g) and was treated conservatively with antihypertensive therapy. Three weeks later, aggravation of the dissection was noted and she was transferred to our hospital, where she underwent an endovascular repair with a tube stent graft (Supporting Table S1).

A physical examination revealed livedo reticularis on both lower legs and iris cysts in both eyes. Her only sibling was a brother (Patient II:1, 32 years old) who suffered an acute aortic dissection (Stanford A type) at the age of 28 years (Fig. 1; Supp. Table S1). He also had iris cysts in both eyes, whereas livedo reticularis was not noted. The aorta in the brother was not evaluated in detail. Her mother (Patient I:2, 56 years old) had the same ocular features, though her aorta was also not evaluated. No affected individuals in this pedigree were noted to have patent ductus arteriosus or bicuspid aortic valves.

The mutation of *ACTA2* found in this patient has been reported in five pedigrees in other studies and is the most common mutation identified thus far. The clinical features of this pedigree were comparable to those depicted in previous reports. Unfortunately, the only DNA sample available for genetic analysis came from the proband.

Family 2

Genomic sequence analysis revealed a heterozygous mutation in the splice donor site of exon 6 (c.616+1G>T) in a male proband (Patient IV:3, index) in Family 2. The transcriptional consequences of this mutation were confirmed by RT-PCR analysis of mRNA from surgical specimens of aortic tissue. RT-PCR using primers for the sequences located in exon 5 and exon 7 showed the existence of a shorter *ACTA2* transcript with deletion of 162 bp (Fig. 2). Direct sequencing for both strands of the RT-PCR product using primers for the sequences located in exon 1 and exon 9 revealed that the 3′ end of exon 5 connected directly to the 5′ end of exon 7, resulting in deletion of the 162-bp portion corresponding

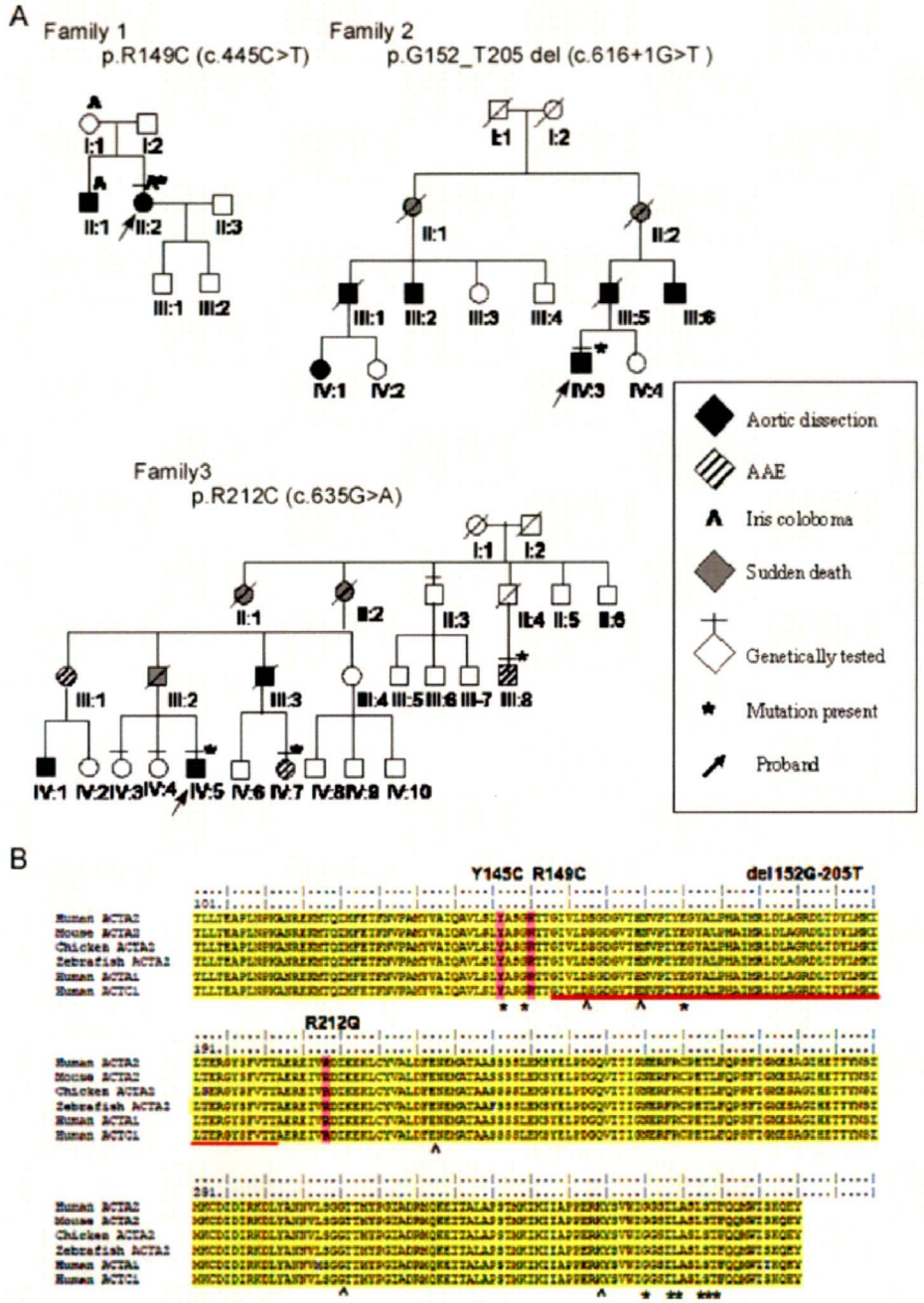

Figure 1. Patient pedigrees and mutations of *ACTA2* gene. **A:** Pedigrees of families with thoracic aortic aneurysms and dissections with *ACTA2* mutations. Individuals with aortic dissections are indicated in black, AAEs are shown in shadows, and sudden deaths are shown in gray. Individuals with iris cysts are indicated with the "^" symbol. Bars indicate individuals genetically tested and asterisks indicate those with *ACTA2* mutations. Arrows indicate probands of the pedigrees. **B:** Locations of the ACTA2 mutations identified in this study are shown with pink blocks or are underlined along with the highly-conserved orthologous protein sequences. Asterisks indicate gelsolin binding sites and arrowheads indicate ATP binding sites.

to the entire exon 6 of the *ACTA2* gene (Fig. 2). This shorter transcript results in an in-frame 54–amino acid deletion from Gly152 to Thr205 (p.G152_T205del), the region extending from subdomains 3 and 4. The mutant peptide was also missing several binding sites for known molecules, including ATP, gelsolin, and profilin, resulting in a completely divergent actin structure [Page et al., 1998; Vorobiev et al., 2003; Dominguez, 2004] (Fig. 3A).

The proband (Patient IV:3) was a 41-year-old male who was presented with an acute aortic dissection (Stanford B type) at the age of 28 years, followed by graft replacement of the descending aorta. At age 40 years, he experienced another acute aortic dissection (Stanford A type), and underwent surgical repair involving the ascending aorta and aortic arch (Supp. Table S1).

The patient had a strong family history of aortic dissection, as 6 out of 12 pedigree members (Patients III:1, III:2, III:5, III:6, IV:1, and IV:3) had experienced an aortic dissection, of whom 1 (Patient II:1) died of heart failure and another (Patient II:2) died suddenly of an unknown etiology at a young age (Fig. 1; Supp.

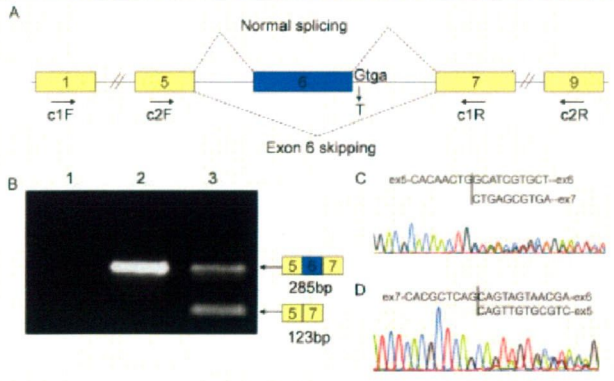

Figure 2. Skipping of exon 6 in *ACTA2* transcript due to genomic mutation in splicing donor site (c.616+1G>T) identified in Family 2. **A:** Schematic diagram of *ACTA2* normal splicing and skipping of exon 6 caused by a mutation in the splice donor site of intron 6. Positions of the primers used for RT-PCR analysis are indicated by arrows. **B:** RT-PCR analysis of *ACTA2* transcripts of the patients. cDNA samples from each patient were amplified with PCR using primers c2F and c1R, as described in (A). Exon 6 skipping and inclusion were assayed using samples from a healthy control (lane 2) and the patient (lane 3). Lane 1 shows a non-reverse-transcribed RNA control. **C,D:** Direct DNA sequence analysis of an RT-PCR fragment (c1F–c2R) representing chimeric cDNA from normal and shorter transcripts. Sequence analysis of both strands confirmed that the shorter transcript was lacking entire exon 6 (162 bp).

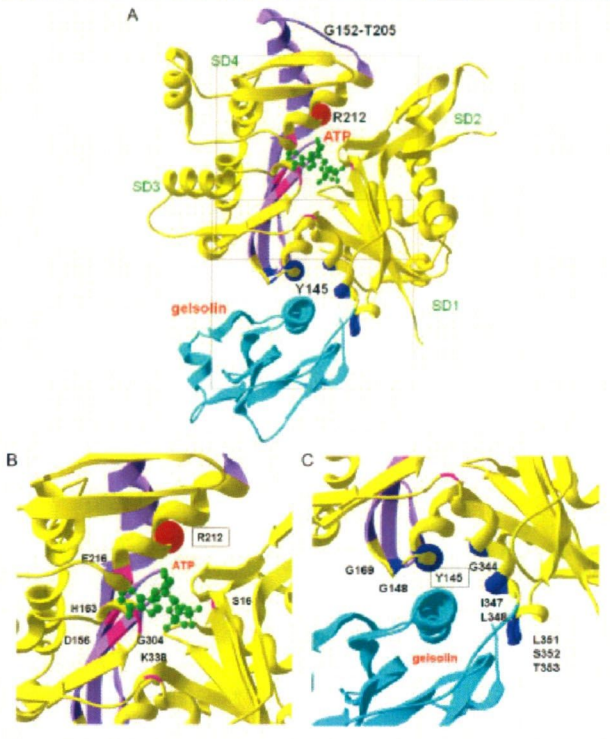

Figure 3. Estimated protein structure and mutations of ACTA2. **A:** ACTA2 monomer domain structure and associated molecules. ATP (shown in green) binding amino acids are shown in pink and gelsolin (shown in light blue) binding amino acids are shown in blue. Locations of the ACTA2 mutations are also mapped. Red and blue spheres represent R212 and Y145, respectively. Amino acids deleted by exon 6 skipping are shown in purple. **B:** Details regarding ATP binding cleft. **C:** Details regarding gelsolin binding interface.

Table S1). The six members had four Stanford A–type aortic dissections, three Stanford B–type aortic dissections, and one undefined type. Since some of the affected individuals were deceased and other family members with or without aortic diseases did not give consent, a genomic DNA sample for genetic analysis was available only from the proband.

The clinical features of this patient were unremarkable, except for early onset of aortic dissection. Although not all members could be closely examined, no ocular, skin, or cardiac abnormalities were noted in any of the remaining individuals.

Family 3

We identified a heterozygous G to A transition at cDNA position 635 in three affected members in Family 3. This mutation is located in exon 6 and predicts an amino acid substitution of Arg212 to Gln. The mutation was not found in the rest of the cohort or in 190 control subjects. Although genetic analysis was performed for three affected members (Patients III:8, IV:5, and IV:7) and three unaffected members (Patients II:3, IV:3, and IV:4), the pedigree chart suggested that the other four affected members (Patients II:1, II:4, III:2, and III:3) would be obligate carriers of this mutation. No mutation was found in any of nonaffected members tested. Arg212 is a highly-conserved amino acid in actin families located in subdomain 4 (Fig. 3B), which faces the ATP binding cleft in the crystallized protein structure and is positioned adjacent to Glu216, one of the known ATP binding sites. Arg212 has also been shown to stabilize the water-mediated hydrogen bonding network across the ATP-binding cleft [Vorobiev et al., 2003]. A substitution of basic Arg212 with a guanidinium side chain to neutral Glu, a side-chain-amide group amino acid, would disturb this stabilization and is expected to be deleterious. We also employed polymorphism phenotyping (PolyPhen) analysis [Ramensky et al., 2002] to predict the impact of the p.R212Q amino acid substitution. The algorithm predicted the substitution would be "probably damaging" because of "disruption of the ligand binding site," with a position-specific independent count (PSIC) score of 2.394 in 496 observations (>2.0 indicated "probably damaging").

The proband (Patient IV-5, index) was a 29-year-old male who was diagnosed with chronic aortic dissection (Stanford B type) at age 25 years, which was followed by a graft replacement of the descending aorta. The onset of dissection was ambiguous, though he had been suffering persistent back pain that started at age 13 years while practicing judo, but was never referred to a hospital. His family history was notable for aortic and vascular diseases (Fig. 1; Supp. Table S1), and he had two relatives, an uncle (Patient III:3) who died of acute dissection of the thoracoabdominal aorta at the age of 45 years and a cousin (Patient IV:1) who experienced aortic dissections at the age of 34 years. Furthermore, his aunt (Patient III:1), another cousin (Patient IV:7), and a first cousin once removed (Patient III:8) had severe or surgically repaired aortic aneurysms. Three other relatives (Patients III:2, II:1, and II:2), including his father, died suddenly of an unknown etiology in their 40 s.

His physical findings were unremarkable, as there were no ocular, skin, or cardiac abnormalities. Echocardiogram results revealed a moderately dilated aortic diameter at the sinuses of Valsalva (left ventricle outflow tract diameter [LVOT] 22 mm, aortic diameter at the sinuses of Valsalva [AoSV] 36 mm, and aortic diameter at the supraaortic ridge [AoSAR] 30 mm).

Two other affected relatives (Patients III:8 and IV:7) were also examined, both of whom had no ocular, skin, or cardiac

abnormalities. Echocardiogram results revealed that Patient III:8 had a dilated aortic diameter at the sinuses of Valsalva (LVOT 23 mm, AoSV 51 mm, AoSAR 44 mm, and aortic diameter at ascending aorta [AoAA] 43 mm). In addition, Patient IV:7 was shown to have a moderately dilated aortic diameter at the sinuses of Valsalva (LVOT 19 mm, AoSV 36 mm, AoSAR 29 mm, and AoAA 30 mm).

Histological examination of surgically removed aortic tissues from Patients IV:5 and IV:7 revealed a disorganized medial fiber structure or cystic medial necrosis (Supp. Fig. S1).

Sporadic Case (M80)

A heterozygous A to G transition at cDNA position 140 in exon 5 of the *ACTA2* gene was detected. This mutation predicts an amino acid substitution of Tyr 145 to Cys, and was not detected in the rest of the cohort or in 190 control subjects. Tyr145 has been shown to be one of the gelsolin binding sites, along with Gly148, Glu169, Gly344, Ile347, Leu348, Leu351, Ser352, and Thr353, and it faces the hydrophobic cleft between subdomains 1 and 4 [Dominguez, 2004] (Fig. 3C). They are all highly-conserved amino acids in the actin family and bind to gelsolin, a key regulator of actin filament assembly and disassembly, by capping and severing F-actin. The substitution of Tyr145 to Cys is expected to perturb the integrity of ligand binding, as shown with previously reported p.R149C and p.T353N (Fig. 3C).

The patient was a 31-year-old male who suffered an acute dissection in the descending aorta (Stanford B type) and was treated conservatively with antihypertensive therapy (Supp. Table S1). He had another acute dissection in the proximal descending aorta 1 year later, followed by graft replacement of the total descending aorta. He became obese (175 cm, 117 kg, body mass index 38.2) after stopping participation in amateur wrestling at the age of 23 years and had mild hypertension, hypercholesterolemia (285 mg/dl), and hyperuricemia (11.8 mg/dl). His family history was unremarkable, and there were no instances of aortic dissection or sudden death. Due to obesity, the echocardiogram examination was incomplete; however, the aortic diameters at the sinuses of Valsalva were not remarkable (AoSV 35 mm, and AoAA 30 mm). Histological examination of surgically removed aortic tissues revealed cystic medial necrosis (Supp. Fig. S1). Unfortunately, physical examination findings and genetic analyses of other family members were unavailable.

Discussion

In the present study, we confirmed that *ACTA2* mutations are an important cause of familial AADs. In a total of 14 probands analyzed, we identified three mutations in three unrelated families, for a ratio of 21%. In a study of a cohort of 97 TAAD families, Guo et al. [2007] argued that *ACTA2* mutations are the most common cause of familial TAAD yet found and are responsible for 14% of reported cases. Our data support their conclusion regarding that point, even though the study design was different. In addition, our analysis of 26 additional sporadic and young-onset TAAD cases identified one mutation that is thought to affect ligand binding characteristics.

Of the four mutations identified in the present study, three were novel. One of these mutations, p.R149C, is the same as reported by Guo et al. [2007] and the clinical presentation was similar, as the patient had livedo reticularis and an iris cyst. The second mutation, c. 616+1G>T, was novel and found to affect mRNA splicing by skipping entire exon 6, resulting in 54 amino acid deletions. It should be unequivocally causative, since a transcribed peptide will lack several important binding sites of known molecules, including ATP, gelsolin, and profilin. The third mutation, p.R212Q, was also novel, and our findings that it affected family members in more than three generations and was located to face the ATP binding cleft suggest it to be a causative mutation. The fourth mutation, p.Y145C, was identified in a nonfamilial case and was also novel. Unfortunately, additional investigations such as a genetic study of his parents could not be performed. Nevertheless, based on the finding showing substitution of gelsolin-binding Tyr, which was previously reported in several structural analyses, we concluded that this mutation was also causative. Although further investigation is needed, we consider that the corresponding *ACTA2* mutation causes deterioration of structural integrity at the cellular level.

We found a higher rate of aortic dissection in the descending portion in patients with the *ACTA2* mutation as compared with previous reports [Guo et al., 2007]. Of 11 dissection events in which the dissection type was proven, six were Stanford type B and five were type A. In the former six patients, at least three were known to be absent of annuloaortic ectasia (AAE) or involvement of the ascending portion of the aorta. This is a significant contrast, since most cases of Marfan syndrome have aortic involvement in the ascending portion, especially the sinus of Valsalva [Boileau et al., 1993; De Paepe et al., 1996; Faivre et al., 2007]. On the other hand, three affected individuals in Family 3 showed only AAE without any dilatation in the descending aorta. In the previous report by Guo et al. [2007], there were 19 aneurysms in the ascending portion, 36 type A dissections, and 13 type B dissections, indicating more type A events than in our study. One possible explanation for this discrepancy is the different mutation types found.

In addition, we found that the extravascular involvements described in the previous report, livedo reticularis and iris folliculi, were rare in our study. Although these features were noted in a patient with the p.R149C mutation, which is the same as in a previous report, no other affected individuals were noted with these features. This may be another mutation-specific feature, since ocular involvements were noted solely with the p.R149C mutation in that previous report.

Interestingly, four patients in our study were former athletes, two tennis players, a judo wrestler, and an amateur wrestler, who actively played sports in their teens before the aortic events occurred. Although there is no evidence, physical contact or higher circulation performance during sports participation might be an additional causative mechanism for aortic events.

While we were revising this report, Guo et al. [2009] reported additional *ACTA2* mutations including p.R212Q in familial TAAD. In addition, they indicated that *ACTA2* mutation carriers can have a diversity of vascular diseases, including premature onset of coronary artery disease and premature ischemic stroke, as well as TAAD. However, we did not find any specific clinical feature suggesting premature onset of coronary artery disease or premature ischemic strokes, though some of family members (Family 2, Patients II:1 and II:2; and Family 3, Patients II:1 and II:2) died suddenly, some with chest pain. Furthermore, we did not find any individual with the *ACTA2* mutation and without aortic disease. Those clinical features require further evaluations using individuals in those families over a long period of time.

In conclusion, our data confirmed that *ACTA2* mutations are important in familial TAAD. Furthermore, we report the first nonfamilial TAAD case with an *ACTA2* mutation. Since the first

and only clinical symptom for these patients was an AAD, which can be life-threatening, identification of mutations in family members of patients with an *ACTA2* mutation would be beneficial in regard to clinical aspects for improved surveillance and awareness of treatment, as well as consideration of social, psychological, and ethical issues. We think that genetic analysis of *ACTA2* for patients with familial TAAD or young-onset TAAD is as clinically as important as that of *FBN1* and *TGFBRs*.

Acknowledgments

We thank Ms. Aya Narita, Ms. Yoko Miyamoto, and other members of the Department of Bioscience for their technical support with this study. We also thank the patients for their participation and members of the Divisions of Cardiovascular Medicine and Surgery for their patient care. This work was supported in part by a Grant for the Promotion of Fundamental Studies in Health Science from the Organization for Pharmaceutical Safety and Research (OPSR) of Japan and a grant from the Program for Promotion of Fundamental Studies in Health Sciences of the National Institute of Biomedical Innovation (NIBIO), as well as Grants-in-Aid for Scientific Research from Japan Society for the Promotion of Science, and Research Grants for Cardiovascular Diseases from the Ministry of Health, Labour and Welfare, Japan.

References

Albornoz G, Coady MA, Roberts M, Davies RR, Tranquilli M, Rizzo JA, Elefteriades JA. 2006. Familial thoracic aortic aneurysms and dissections—incidence, modes of inheritance, and phenotypic patterns. Ann Thorac Surg 82:1400–1405.

Biddinger A, Rocklin M, Coselli J, Milewicz DM. 1997. Familial thoracic aortic dilatations and dissections: a case control study. J Vasc Surg 25:506–511.

Boileau C, Jondeau G, Babron MC, Coulon M, Alexandre JA, Sakai L, Melki J, Delorme G, Dubourg O, Bonaiti-Pellie C, Bourdarias JP, Junien C. 1993. Autosomal dominant Marfan-like connective-tissue disorder with aortic dilation and skeletal anomalies not linked to the fibrillin genes. Am J Hum Genet 53:46–54.

Coady MA, Davies RR, Roberts M, Goldstein LJ, Rogalski MJ, Rizzo JA, Hammond GL, Kopf GS, Elefteriades JA. 1999. Familial patterns of thoracic aortic aneurysms. Arch Surg 134:361–367.

De Paepe A, Devereux RB, Dietz HC, Hennekam RC, Pyeritz RE. 1996. Revised diagnostic criteria for the Marfan syndrome. Am J Med Genet 62:417–426.

Dietz HC, Cutting GR, Pyeritz RE, Maslen CL, Sakai LY, Corson GM, Puffenberger EG, Hamosh A, Nanthakumar EJ, Curristin M, Stetten G, Meyers DA, Francomano CA. 1991. Marfan syndrome caused by a recurrent de novo missense mutation in the fibrillin gene. Nature 352:337–339.

Dominguez R. 2004. Actin-binding proteins—a unifying hypothesis. Trends Biochem Sci 29:572–578.

Faivre L, Collod-Beroud G, Loeys BL, Child A, Binquet C, Gautier E, Callewaert B, Arbustini E, Mayer K, Arslan-Kirchner M, Kiotsekoglou A, Comeglio P, Marziliano N, Dietz HC, Halliday D, Beroud C, Bonithon-Kopp C, Claustres M, Muti C, Plauchu H, Robinson PN, Adès LC, Biggin A, Benetts B, Brett M, Holman KJ, De Backer J, Coucke P, Francke U, De Paepe A, Jondeau G, Boileau C. 2007. Effect of mutation type and location on clinical outcome in 1,013 probands with Marfan syndrome or related phenotypes and *FBN1* mutations: an international study. Am J Hum Genet 81:454–466.

Garg V, Muth AN, Ransom JF, Schluterman MK, Barnes R, King IN, Grossfeld PD, Srivastava D. 2005. Mutations in *NOTCH1* cause aortic valve disease. Nature 437:270–274.

Guex N, Peitsch MC. 1988. SWISS-MODEL and the Swiss-PdbViewer: an environment for comparative protein modeling. Electrophoresis 18:2714–2723.

Guo DC, Pannu H, Tran-Fadulu V, Papke CL, Yu RK, Avidan N, Bourgeois S, Estrera AL, Safi HJ, Sparks E, Amor D, Ades L, McConnell V, Willoughby CE, Abuelo D, Willing M, Lewis RA, Kim DH, Scherer S, Tung PP, Ahn C, Buja LM, Raman CS, Shete SS, Milewicz DM. 2007. Mutations in smooth muscle alpha-actin (ACTA2) lead to thoracic aortic aneurysms and dissections. Nat Genet 39:1488–1493.

Guo DC, Papke CL, Tran-Fadulu V, Regalado ES, Avidan N, Johnson RJ, Kim DH, Pannu H, Willing MC, Sparks E, Pyeritz RE, Singh MN, Dalman RL, Grotta JC, Marian AJ, Boerwinkle EA, Frazier LQ, LeMaire SA, Coselli JS, Estrera AL, Safi HJ, Veeraraghavan S, Muzny DM, Wheeler DA, Willerson JT, Yu RK, Shete SS, Scherer SE, Raman CS, Buja LM, Milewicz DM. 2009. Mutations in smooth muscle alpha-actin (ACTA2) case coronary artery disease, stroke, and Moyamoya disease, along with thoracic aortic disease. Am J Hum Genet 84:617–627.

Loeys BL, Chen J, Neptune ER, Judge DP, Podowski M, Holm T, Meyers J, Leitch CC, Katsanis N, Sharifi N, Xu FL, Myers LA, Spevak PJ, Cameron DE, De Backer J, Hellemans J, Chen Y, Davis EC, Webb CL, Kress W, Coucke P, Rifkin DB, De Paepe AM, Dietz HC. 2005. A syndrome of altered cardiovascular, craniofacial, neurocognitive and skeletal development caused by mutations in *TGFBR1* or *TGFBR2*. Nat Genet 37:275–281.

Mizuguchi T, Collod-Beroud G, Akiyama T, Abifadel M, Harada N, Morisaki T, Allard D, Varret M, Claustres M, Morisaki H, Ihara M, Kinoshita A, Yoshiura K, Junien C, Kajii T, Jondeau G, Ohta T, Kishino T, Furukawa Y, Nakamura Y, Niikawa N, Boileau C, Matsumoto N. 2004. Heterozygous *TGFBR2* mutations in Marfan syndrome. Nat Genet 36:855–860.

Page R, Lindberg U, Schutt CE. 1998. Domain motions in actin. J Mol Biol 280:463–474.

Pannu H, Avidan N, Tran-Fadulu V, Milewicz DM. 2006. Genetic basis of thoracic aortic aneurysms and dissections: potential relevance to abdominal aortic aneurysms. Ann NY Acad Sci 1085:242–255.

Pannu H, Tran-Fadulu V, Papke CL, Scherer S, Liu Y, Presley C, Guo D, Estrera AL, Safi HJ, Brasier AR, Vick GW, Marian AJ, Raman CS, Buja LM, Milewicz DM. 2007. MYH11 mutations result in a distinct vascular pathology driven by insulin-like growth factor 1 and angiotensin II. Hum Mol Genet 16:2453–2462.

Ramensky V, Bork P, Sunyaev S. 2002. Human non-synonymous SNPs: server and survey. Nucleic Acids Res 30:3894–3900.

Superti-Furga A, Gugler E, Gitzelmann R, Steinmann B. 1988. Ehlers-Danlos syndrome type IV: a multi-exon deletion in one of the two COL3A1 alleles affecting structure, stability, and processing of type III procollagen. J Biol Chem 263:6226–6232.

Vorobiev S, Strokopytov B, Drubin DG, Frieden C, Ono S, Condeelis J, Rubenstein PA, Almo SC. 2003. The structure of nonvertebrate actin: implications for the ATP hydrolytic mechanism. Proc Natl Acad Sci USA 100:5760–5765.

Zhu L, Vranckx R, Van Kien PK, Lalande A, Boisset N, Mathieu F, Wegman M, Glancy L, Gasc JM, Brunotte F, Bruneval P, Wolf JE, Michel JB, Jeunemaitre X. 2006. Mutations in myosin heavy chain 11 cause a syndrome associating thoracic aortic aneurysm/aortic dissection and patent ductus arteriosus. Nat Genet 38:343–349.

TEN-2009-0218-Miskon_1P
Type: research-article

TISSUE ENGINEERING: Part C
Volume 00, Number 00, 2010

DOI: 10.1089/ten.tec.2009.0218

Methods Article

A Suspension Induction for Myocardial Differentiation of Rat Mesenchymal Stem Cells on Various Extracellular Matrix Proteins

Azizi Miskon, M.Eng.,[1–3] Atsushi Mahara, Ph.D.,[1] Hiroshi Uyama, Ph.D.,[2] and Tetsuji Yamaoka, Ph.D.[1,4]

AU1 ▶ The microenvironment of bone marrow-derived mesenchymal stem cells (MSCs) strictly regulates their differentiation. In this study, we have developed a new suspension induction method for myocardial differentiation of bone marrow-derived rat MSCs (rMSCs) *in vitro* on various extracellular matrix (ECM) proteins. Myocardial differentiation of rMSCs was induced with a conventional monolayer method and our suspension method. In our suspension induction, a cell suspension was treated with the medium in the presence of an inducer, incubated for 2 h under a suspension conditions, and moved to a monolayer culture on gelatin-coated, collagen type I-coated, fibronectin-coated, or polystyrene dishes until the total induction time was 24 h. We evaluated the myocardial differentiation by counting the number of colonies of beating cells, performing immunohistochemical staining, and measuring the expression of cardiac-specific gene mRNA using real-time quantitative polymerase chain reaction. We found that rMSCs induced with the conventional monolayer method did not differentiate efficiently, whereas beating cell colonies were found on ECM-coated dishes of suspension-induced cells, after 3 weeks of culture, especially on gelatin-coated dishes. The beating cells were positively stained with anti-troponin T-C antibody and expressed specific cardiac markers. In conclusion, these results demonstrated that the suspension induction followed by subsequent culture on gelatin ECM substrates is a promising method for differentiating rMSCs into cardiomyocytes *in vitro*.

Introduction

ISCHEMIC HEART DISEASE is the primary cause of death throughout the world.[1] Adult cardiac muscle, unlike skeletal muscle, lacks the ability to regenerate after ischemic injury. The only eventual therapy is cardiac transplantation. However, this option is limited by a lack of donor organs.

An implantable left ventricular assist device has been proposed as a bridge to transplant for many patients who are on a waiting list for donor organs.[2] Left ventricular assist device can improve organ perfusion, reduce wall stress, and improve functional capacity and quality of life, but it is not an option for the majority of people with heart failure.[3,4] Thus, the ultimate goal is to repair the injured myocardium by cell transplantation.

Some fundamental studies and clinical trials suggest that cell-based therapies can improve cardiac function.[5–8] The isolation of cardiomyocytes from a patient's heart is unrealistic at present. In general, three types of potential cell sources have been proposed, but the search for these sources and types of cells are still under investigation.[9] One potential source is allogeneic cells, including human embryonic stem cells or fetal allogeneic cardiomyocytes, but there remain ethical issues in their use. Another option is transgenic sources. Genetically engineered animal cardiomyocytes have been studied in an attempt to reduce the rejection reaction *in vivo*, which is still a long-term problem in recipients.[9]

To deal with this problem, autograft bone marrow-derived mesenchymal stem cells (MSCs) are foreseen to be the most promising candidate for transplantation, because they are easy to obtain and less immunogenic than other stem cells. The differentiation of MSCs into cardiomyocytes *in vivo* has been observed, but it occurs at an extremely low rate and its efficiency is under debate.[7,10]

The production of autologous beating cardiomyocytes is thus an attractive goal for cell-based therapy. For this purpose, it is preferable to differentiate MSCs into cardiomyocytes

[1]Department of Biomedical Engineering, Advanced Medical Engineering Center, National Cardiovascular Center Research Institute, Osaka, Japan.
[2]Department of Chemical Engineering, Osaka University, Osaka, Japan.
[3]Department of Electronic Engineering, Faculty of Electrical and Electronics Engineering, University Tun Hussein Onn Malaysia, Johor, Malaysia.
[4]JST, CREST, Tokyo, Japan.

in vitro before transplantation, and it is crucial to understand how best to achieve this.

Based on traditional isolation of MSCs and monolayer culture, Wakitani *et al.* reported that rat MSCs (rMSCs) were differentiated to myogenic cells after 24 h of exposure to DNA-demethylating agent 5-azacytidine,[10] and Makino *et al.* reported that the repeated treatment of murine MSCs with 5-azacytidine differentiated the cells into cardiomyocytes with high cardiac marker expression *in vitro*.[11] These findings are in contrast with a report that functional cardiac cells and gene expression were not obtained after treatment with 5-azacytidine.[12] Wang *et al.* also reported cardiac marker expression in 5-azacytidine-treated MSCs, but they did not observe any beating cells.[13] The differences in these observations might be related to the efficiency of the inducer and the timing of induction.

Clemmons *et al.* reported that fibroblasts in the suspension did not undergo DNA synthesis and division.[14] Griffin and Houstan reported that cells in monolayer cultures are in a static environment and have a relatively small surface area for diffusion, in contrast to suspension cultures in which the entire surface area is exposed to the drug.[15] In addition, in suspensions, efflux transporters are not retained because of the loss of cell polarity and redistribution of canalicular membranes[16]; therefore, the compound remains in the cell. Hence, we assumed that by treating the cells with the inducer in suspension culture, the treated cells were more likely to proceed toward the differentiation phase instead of the division phase.

Langer and Vacanti reported that three important components of tissue-engineered constructs were the cell source, soluble chemical factor, and extracellular matrix (ECM).[17] ECM proteins and the cooperation between signaling pathways triggered by soluble factors such as growth and differentiation factors were found to determine cell proliferation and cell differentiation.[18] In our previous study, ECM components were seen to affect the beating behavior of primary neonatal cardiomyocytes and cardiac differentiated P19.CL6 cells in which enhanced beating behavior and cardiac differentiation on gelatin-coated dishes were observed.[19]

The aim of our studies was to produce spontaneously beating cardiac cells from rMSCs by our new induction method on different substrates. Optimal substrates for stem cell attachment, proliferation, and differentiation have been reported for various types of stem cells.[20] In this study, treated rMSCs were cultured on gelatin-coated, fibronectin-coated, collagen type I-coated, and polystyrene dishes. We treated rMSCs using a newly established suspension method, and the differentiation tendency was compared with those treated by the conventional monolayer method.

Materials and Methods

Bone marrow cell preparation

Femora and tibiae of 4-week-old, male Sprague Dawley rats with average body weight of 80 g were collected and adherent soft tissues were removed. Institutional guidelines for the care and use of laboratory animals were observed. The rMSCs were obtained from collected femora and tibiae by flushing the marrow cavities. Isolated cells were cultured in high-glucose Dulbecco's modified Eagle's medium (DMEM-HG; Gibco, Grand Island, NY) supplemented with 10% fetal bovine serum (lot no. 7297H; MP Biomedicals, Eschwege, Germany), 5% heat-inactivated horse serum (lot no. 076K8430; Sigma-Aldrich, St. Louis, MO), and penicillin (100 U/mL)/streptomycin (100 μg/mL) (Wako, Osaka, Japan).

The cells were seeded on 10 mm fibronectin-coated dishes (BD Falcon, BD BioCoat, BD Biosciences, Bedford, MA) and incubated in a 5% carbon dioxide (CO_2)/air atmosphere at 37°C. At 24 h after plating, nonadherent cells were removed, and the medium was changed every 3 days until the adherent cells reached 80% confluence. The cells in one dish were harvested with 0.25 mg/mL trypsin (Lonza, Walkersville, MD), washed with phosphate-buffered saline (PBS), and seeded onto three new dishes.

Isolation of neonatal heart

Cardiomyocytes were isolated from neonatal (2-day-old) Sprague Dawley rat hearts by the collagenase digestion method with modifications.[21,22] Institutional guidelines for the care and use of laboratory animals were followed. The hearts were removed and carefully minced with a scalpel blade into fragments and rinsed several times with Hanks' balanced salt solution (Sigma-Aldrich) to remove blood and cellular debris. The minced hearts were gently stirred in 50 mL collagenase solution (0.15 M NaCl, 5.63 mM KCl, 0.02 M HEPES, 0.02 M $NaHCO_3$, 3.74 mM $CaCl_2 \cdot 2H_2O$, and 6.5×10^4 U collagenase [lot no. 06032W; Wako]) at 37 C for 30 min. The resulting cell suspension was filtered through a 40 μm pore-sized nylon cell strainer (BD Falcon, BD BioCoat, BD Bioscience) and centrifuged at 78 *g* for 3 min.

Isolated cardiomyocytes were cultured in minimum essential medium alpha (Gibco) supplemented with 10% (v/v) fetal bovine serum (lot no. 7297H; MP Biomedicals) and 100 IU/L penicillin–streptomycin (Wako) on 60 mm gelatin-coated dishes (Iwaki; Asahi Glass, Tokyo, Japan). Three days after isolation the mRNA levels of the cardiac marker genes were evaluated.

Cardiomyocyte differentiation

Monolayer induction. The rMSCs at fourth passage were seeded on 60 mm gelatin-coated dishes (Iwaki; Asahi Glass), fibronectin-coated dishes (BD Falcon, BD BioCoat, BD Biosciences), collagen type I-coated dishes, and noncoated polystyrene dishes (Iwaki; Asahi Glass) at a density of 1.0×10^5 cells/dish. The cells were cultured at 37°C in humidified air with 5% CO_2, reaching 80% confluence within 3 days. Afterward the cells were exposed to the inducers, 10 μM 5-azacytidine (Nacalai Tesque, Kyoto, Japan), 300 μM L-ascorbic acid phosphate magnesium salt *n*-hydrate (Wako), and 0.025 μg/mL human basic fibroblast growth factor (Sigma-Aldrich)-containing DMEM-HG for 24 h. Then, the inducers were washed away and cells were cultured for 5 weeks with DMEM-HG without inducers to develop the beating cells. The medium was changed every 3 days. The cell morphologies were observed every day using Nikon Eclipse TE 300 (Nikon, Tokyo, Japan) light microscope. An image was taken after 3 weeks of cultivation using Image Pro 4.5 software (Media Cybernetics, Silver Spring, MD).

Suspension induction. The suspension of 1.0×10^5 rMSCs was treated with and without 10 μM 5-azacytidine (Nacalai

Tesque), 300 μM L-ascorbic acid phosphate magnesium salt *n*-hydrate (Wako), and 0.025 μg/mL human basic fibroblast growth factor (Sigma-Aldrich)-containing DMEM-HG in a floating condition in a centrifuge tube (Iwaki; Asahi Glass) for 2 h at 37°C in humidified air with 5% CO_2. The treated cells were cultured on 60 mm gelatin-coated dishes (Iwaki; Asahi Glass), fibronectin-coated dishes (BD Falcon, BD BioCoat, BD Biosciences), collagen type I-coated dishes, and noncoated polystyrene dishes (Iwaki; Asahi Glass) in the presence of inducers until the total induction time was 24 h, then with DMEM-HG without inducers for 5 weeks. The medium was changed every 3 days. The cell morphologies were examined every day using a Nikon Eclipse TE 300 (Nikon) light microscope. Images were taken after 3 weeks of cultivation using Image Pro 4.5 software (Media Cybernetics).

The experiments were repeated to determine the expression of troponin C type-2 after suspension induction.

Total RNA isolation and reverse transcription

Total cellular RNAs from both noninduced and induced rMSCs with monolayer induction and suspension induction were extracted by QuickGene RNA cultured cell kit S (Fujifilm Life Science, Tokyo, Japan) after 1, 2, and 3 weeks of culture. In another experiment, total cellular RNAs from induced rMSCs with suspension induction were extracted after 1, 2, 3, 4, and 5 weeks. The cellular RNAs from neonatal cardiomyocytes were also extracted with the same protocol after 3 days of culture as a positive control for real-time quantitative polymerase chain reaction (PCR). Total cellular RNAs were calculated as follows: [RNA] = A_{260} (nm) × Dilution × 40 μg/mL. The RNAs from beating and nonbeating colonies were extracted separately.

First-strand cDNAs were synthesized using a mixture of oligo(dT)$_{18}$ primer. Total cellular RNAs (200 ng) were incubated with 2.5 μM oligo(dT)$_{18}$ primer at 70°C for 10 min to denature RNA secondary structure and then incubated at 4°C to let the primer anneal to the RNA. A given amount of 5× RT buffer (Toyobo, Osaka, Japan) and 2.5 mM dNTP mixture (Takara Bio, Shiga, Japan) (4 μL) were added and incubated at 37°C for 5 min. Reverse transcriptase (100 units; Toyobo) was added into the mixture and the RT reaction was extended at 37°C for 1 h. Then the reaction was heated at 94°C for 5 min to inactivate the enzyme and cooled at 4°C for 15 min. RNase (DNase-free, 0.5 μg; Roche Diagnostics GmbH, Mannheim, Germany) was added into the mixture and incubated at 37°C to remove the template RNA. To confirm that the beating cells were cardiomyocytes, an immunochemical study was conducted, in which the expressions of cardiac-specific markers (TNNC 1, TNNT 2, TNNI 3, GATA 4, and MEF2D) were measured.

Real-time quantitative PCR

Real-time quantitative PCR was conducted with SYBR Green. Primers for PCR analysis of troponin T type-2 (cardiac) (TNNT 2), troponin C type-1 (slow) (TNNC 1), troponin I type-3 (cardiac) (TNNI 3), GATA4, MEF2D, and troponin C type-2 (fast) (TNNC 2) were designed using Primer Express software (Perkin-Elmer Applied Biosystems, Warrington, UK). Primer sequences are shown in Table 1. The reaction mixtures contained 23.74 μL distilled water, 25 μL SYBR Green Real-Time PCR master mix (Toyobo), 100 nM of each

TABLE 1. POLYMERASE CHAIN REACTION PRIMERS USED IN THIS STUDY

Genes	Sense	Position (bp)	Antisense	Position (bp)	Accession no.
TNNT 2	5′-GAAACAGGATCAACGACAACCA-3′	827–848	5′-CGCCCGGTGACTTTGG-3′	875–890	NM_012676
TNNC 1	5′-GATCTCTTCCGCATGTTTGACA-3′	295–316	5′-TGGCCTGCAGCATCATCTT-3′	352–370	NM_001034105
TNNI 3	5′-CCAGGAATCTGCAATCCCATT-3′	65–85	5′-CCGCATCCCTGCTCTCA-3′	114–130	NM_017144
TNNC 2	5′-AGATCGAATCCCTGATGAAGGA-3′	392–413	5′-CATCTTCAGAAACTCGTCGAAGTC-3′	442–465	NM_001037351
GATA 4	5′-CAGTTCTGCACACCTGTATTCCA-3′	452–474	5′-GCTCCCCTTTATTTGCAAGTCA-3′	515–536	NM_144730
MEF2D	5′-GCGGCTGGATACTTGGACATT-3′	1251–1271	5′-CGGTGAGATTGTCAACTCTTCATC-3′	2009–2032	NM_030860
GAPDH	5′-CTACCCCCAATGTATCCGTTGT-3′	742–763	5′-TAGCCCAGGATGCCCTTTAGT-3′	842–862	AB017801

primer, and 0.26 μL cDNA. The thermal profile for PCR was 50°C for 2 min, followed by 95°C for 10 min, and then 40 cycles of 15 s at 95°C and 1 min at 60°C. We also performed a negative control PCR reaction using 0.26 μL distilled water to ensure the absence of template contamination in PCR reagents. The cycle number at which the reaction crossed an arbitrarily placed threshold (Cτ) was determined for each gene. The average Cτ values of triplicate measurements were used for all subsequent calculations on the basis of the delta Ct method (ΔCτ). The amount of mRNA levels was determined by $2^{\Delta C_T}$. To correct any variation in mRNA content, the quantities of the genes of interest were normalized by the quantity of glyceraldehyde-3-phosphate dehydrogenase and expressed as relative values of mRNA.

Immunostaining analysis

To confirm the protein expression in addition to the mRNA expression, cells generated by the monolayer method and beating cells generated by suspension induction were stained with anti-troponin T-C antibody. After 4 weeks of culture, the cells were fixed with 10% formalin in PBS and washed with PBS three times. Next, the cells were incubated for 5 min in 0.1% hydrogen peroxide in PBS to quench endogenous peroxide activity and washed in PBS twice for 5 min each. Then the cells were incubated with 10% block-ACE (Dainippon Sumitomo Pharma, Osaka, Japan) in PBS for 20 min to suppress nonspecific binding of IgG. After three cycles of washing with PBS for 5 min each, the cells were incubated with 2.5 μL/mL primary antibody (troponin T-C(C-19), sc-8121; Santa Cruz Biotechnology, CA) for 60 min in PBS with 1.5% block-ACE, washed three times in PBS for 5 min, and incubated with 2 μL/mL secondary antibody (donkey anti-goat IgG-FITC, sc-8121; Cosmo Bio, Tokyo, Japan) for 45 min in PBS with 1.5% block-ACE. The cells were washed with PBS four times and mounted with aqueous mounting medium.

Stained cells were observed using Nikon Eclipse TE 300 (Nikon) fluorescence microscope. An image was taken using Image Pro 4.5 software (Media Cybernetics) with the following parameters: for bright file, an exposure time of 20 ms and gain of 7; for fluorescence, an exposure time of 2 s and gain of 7.

Statistical analysis

All data are presented as means ± standard deviations. Statistical analysis was performed using Student's *t*-test. A *p*-value of less than 0.05 was considered significant.

Results

rMSCs form myotubes

After 3 weeks of cultivation, the shape of the cells induced with suspension induction was very different from that with monolayer induction, as shown in Figure 1. The shape of the suspension-induced cells appeared to be myotubular and seemed to correlate closely to beating colony formation. The phenotypic difference in these shapes was confirmed by measuring TNNT 2, TNNC 1, and TNNC 2 expression.

Expression of cardiomyocyte-associated genes in monolayer and suspension induction

Troponin T type-2 (cardiac, TNNT 2) and troponin C type-1 (slow, TNNC 1) are known to be markers of cardiomyocytes,[23,24] and troponin C type-2 (fast, TNNC 2) is reported to be expressed at the early stage of the cardiac development.[23] In this study, the expression of TNNT 2 was higher in the suspension induction than in the monolayer induction, as shown in Figure 2A. On the other hand, TNNC 1 expression was generally lower in the suspension induction than in the monolayer induction (Fig. 2B). However, the gene expression of TNNC 2 was detected only in the suspension induction and not in the monolayer induction (Fig. 2C). These results indicate that the suppression of TNNC 1 may have been affected by the expression of TNNC 2 and signify the initial stage of cardiac differentiation, as suggested by Stoutamyer and Dhoot.[23] In addition, the gene expression of TNNT 2 and TNNC 2 were detected only in rMSCs treated with inducers and not in the rMSCs treated without inducers (Supplemental Fig. S1 available online at www.liebertonline.com). The expression level of TNNC 1 was generally higher in the treated rMSCs with inducers than in the treated rMSCs without inducers.

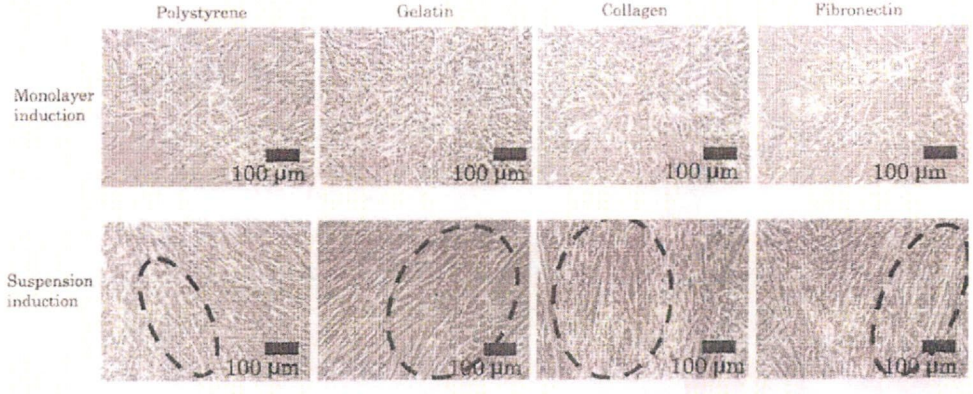

FIG. 1. Microscopic image of rMSCs after monolayer or suspension induction and 3 weeks of culture on several types of dishes. Dashed regions represent the regions of cells with myotube-like shape. rMSC, rat mesenchymal stem cell.

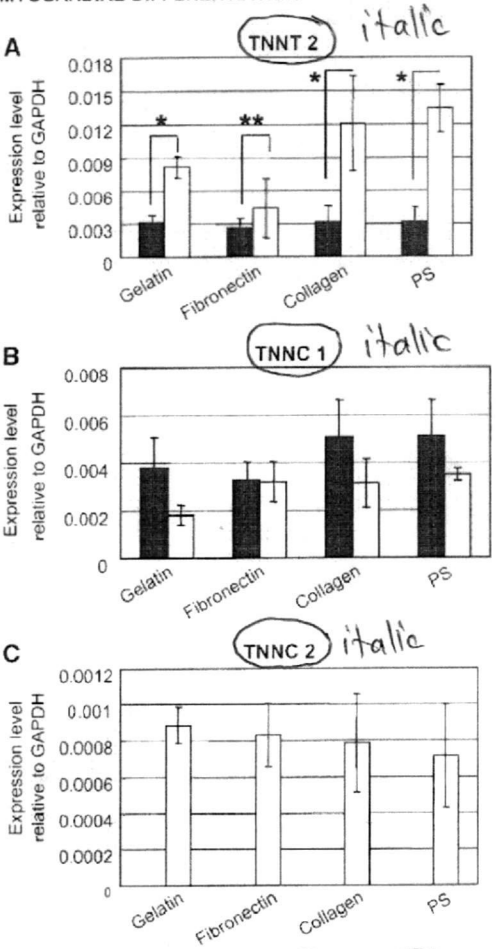

FIG. 2. Expression levels of (A) TNNT 2, (B) TNNC 1, and (C) TNNC 2 in cells after monolayer (■) or suspension induction (□) and culture on different extracellular matrix proteins or uncoated polystyrene dishes ($n = 3$; bars represent ± standard deviation; $^{*}p < 0.01$, $^{**}p < 0.16$).

In other experiments, the expression of TNN2 was detected after 2 weeks of differentiation and decreased by culture time as shown in Figure 3. This observation is possibly related to the cardiomyocyte differentiation. Besides, this result shows similarity with that during quail heart development *in ovo*.[23]

Myotube-like cells on ECM substrates show spontaneous contraction

In general, about 3 weeks are needed to observe spontaneous beating of the cells without the addition of any chemical reagent, such as acetylcholine.[10,25] Once the beatings are detected, it takes about another 1 week to enter the synchronous stage.

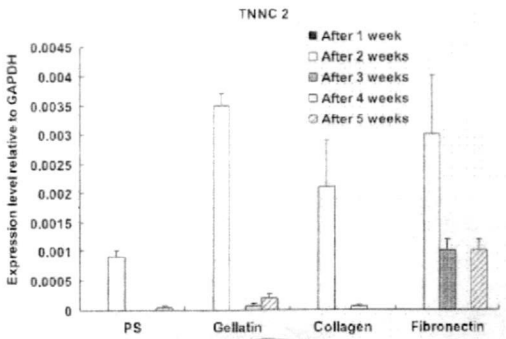

FIG. 3. The expression of TNNC 2 decreased with culture period. Data are means ± standard deviation; $n = 3$ for each sample.

Interestingly, the beating cells and colonies were detected only after they were induced with suspension induction on ECM protein-coated dishes, but not in monolayer induction. We carried out these induction experiments 14 times and found a beating colony only once in monolayer induction on gelatin-coated dishes. As five dishes were used for each experiment, the average number of beating colonies in one dish was calculated as 0.75 ± 1.5 (Table 2). However, the real probability of beating colony appearance was much lower than this value. A large number of beating colonies (4.5 ± 0.6) with sizes ranging from 400 to 500 μm were found in the five gelatin-coated dishes, and 1.3 ± 1.5 beating colonies with a similar size were found in the five fibronectin-coated and collagen type-I-coated dishes. No beating cells were detected in noncoated polystyrene dishes in either form of induction. Table 2 summarizes the colonies of beating cells. Supplemental Video S1 (available online at www.liebertonline.com) shows the beating colonies after 4 weeks of culture on gelatin-coated dishes.

In some cases, monolayer-treated and suspension-treated rMSCs were detached from the dishes after 3 weeks of culture. The nondetached cells proliferated and only suspension-treated rMSCs became beating cells after 6 weeks of culture (data not shown).

Immunostaining

Immunofluorescence examination clearly showed that when the dishes were stained with anti-troponin T-C

TABLE 2. AVERAGE NUMBER OF BEATING COLONIES FOUND IN A DISH (n = 5)

	Average number of beating colonies per dish	
Dish type	*Monolayer*	*Suspension*
Gelatin	0.75 ± 1.5	4.5 ± 0.6
Fibronectin	0	1.3 ± 1.5
Collagen type I	0	1.3 ± 1.5
Polystyrene	0	0

Five 60 mm culture dishes were used for calculation of average beating colony number.

antibody, the beating areas were positively stained as shown in Figure 4, but cells treated by monolayer induction remained at the background level of staining.

Expression of cardiomyocyte-associated genes in beating and nonbeating cells

To define the phenotype of the beating cells, the expression levels of cardiac-specific genes (TNNC 1, TNNT 2, TNNC 2, TNNI 3, GATA 4, and MEF2D) were evaluated. Expression levels of given genes were assessed using RNAs from neonatal hearts as positive qualitative controls. The expression levels of TNNC 1, TNNT 2, and MEF2D were higher in beating cells than in nonbeating cells, as shown in Figure 5A and B. The expressions of TNNI 3 and GATA 4 were detected in only one of four isolated colonies of beating cells and were not detected in any nonbeating colonies. The high expression of TNNC2 in Figure 5A is possibly because either skeletal muscle cells or initial cardiomyocytes are also present in the beating colonies.

In neonatal cardiomyocytes (3 days of cultivation), TNNC 1, TNNT 2, TNNI 3, and GATA 4 were expressed (Fig. 5A, B). However, TNNC 2 was not expressed. These data suggested that 25% of the beating cells were cardiomyocytes and 75% were late-maturing cardiomyocytes.

Discussion

MSCs derived from bone marrow are useful cells because they can be isolated from patients and can differentiate into many types of cells. The production of autologous beating cardiomyocytes is an attractive goal for cell-based therapy. However, in previous studies, differentiation into cardiomyocytes occurred at extremely low rates.[7,10] Therefore, it is essential to establish a new, more effective system for differentiating MSCs into beating cardiomyocytes *in vitro* before being transplanted into patients. Other reports have demonstrated that rat and mouse bone marrow cells can differentiate into cardiomyocytes *in vitro*.[10,11] On the other hand, Liu *et al.* reported that 5-azacytidine could not expand rMSCs or induce their differentiation into cardiomyocytes.[12] In our experience from 14 experiments in suspension and monolayer induction, beating cells were obtained in only 7 experiments with suspension induction and in 1 with monolayer induction. These results suggested that beating cardiomyocytes were not easily obtained after exposure to 5-azacytidine. In this regard, the induction method and the substrate are important to obtain beating cardiomyocytes.

Some reports have described manipulating microenvironmental factors, such as cell dimensions, controlled delivery of soluble factors, chemical cues, mechanical cues, and culture substrates, for the controlled differentiation of stem cells.[26,27] Cells in monolayer culture are in a static environment and have a relatively small surface area for diffusion in contrast to cells in suspension culture.[15] In this study, more than 90% of cells induced with suspension method were adhered onto the dishes at 24 h after the cells were inoculated into monolayer cultures (Supplemental Fig. S2 available online at www.liebertonline.com). After 3 weeks in culture, the cells induced by the suspension method were shaped like myotubes on all types of dishes, as shown in Figure 1, and had begun to form colonies. These differentiated myotube shapes were similar to those described by Wakitani *et al.* and Makino *et al.*

In this study, the expression of TNNT 2 was higher in suspension induction than in monolayer induction, as shown in Figure 2A. On the other hand, TNNC 1 expression was generally lower in suspension induction than in monolayer induction (Fig. 2B). However, the gene expression of TNNC 2 was detected only with the suspension induction and not with the monolayer induction (Fig. 2C). These results indicated that differentiation efficiency was affected by suspension induction. The enhancement mechanism is unclear but may be related to the proliferation activity, which had not yet started in the suspension condition.

The expression levels of cardiac-specific genes (TNNT 2, TNNC 1, and MEF2D) of the beating cells were higher than those of nonbeating cells and almost the same level as those of neonatal cardiomyocytes. The beating of neonatal cardi-

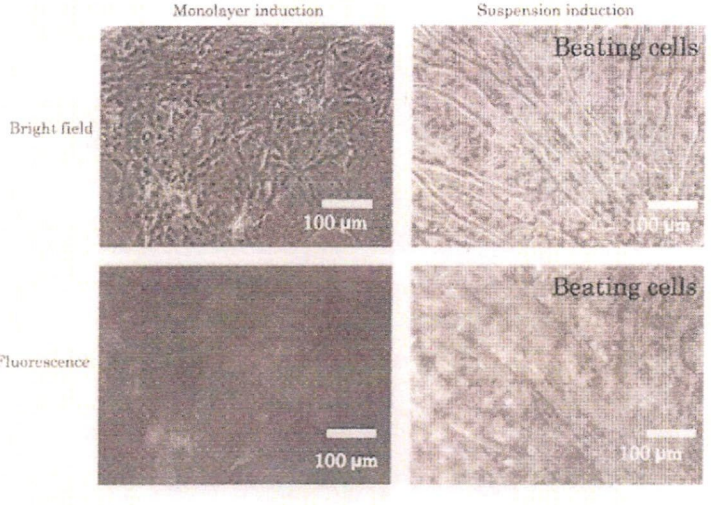

FIG. 4. rMSCs induced by monolayer or suspension method were stained with anti-troponin I-C antibody.